Title

Antimicrobial Peptides as a Potential Mechanism for Bacterially Induced Metamorphosis of the Sea Urchin Lytechinus pictus

Author

Hargadon, Alexis Cody

Publication Date

2023

Peer reviewed|Thesis/dissertation

UNIVERSITY OF CALIFORNIA SAN DIEGO

Antimicrobial Peptides as a Potential Mechanism for Bacterially Induced Metamorphosis of the Sea Urchin *Lytechinus pictus*

A Thesis submitted in partial satisfaction of the requirements
for the degree Master of Science

in

Marine Biology

by

Alexis Cody Hargadon

Committee in charge:

Professor Amro Hamdoun, Chair
Professor Paul Jensen
Professor Deidre Lyons

2023

The Thesis of Alexis Cody Hargadon is approved, and it is acceptable in quality and form for publication on microfilm and electronically.

University of California San Diego

2023

DEDICATION

I've spent a lot of time in Hubbs Hall by now. I'd like to thank everybody I've crossed paths with over the last (almost) 5 years for inspiring me to do hard things. Here are just a few.

Thank you to Tim Healy, my first mentor in research. You always knew the right way to not only teach me (not an easy task), but to be there for me. Thank you for supporting my independence and understanding my stubbornness. I would not be the scientist or person I'm today without you. To the rest of the Burton lab, thank you for some of my best friends. My undergraduate memories will forever be dominated by our adventures.

To the badass Professor Catherine Schrankel, who really was not obligated to continue to mentor me while starting the Schrankel lab at SDSU. Words cannot describe how grateful I am for you. You will always be my inspiration to remain enthusiastic, creative, and determined.

Amro, thank you for letting me come into your office and tell you what I wanted to do. And thank you for always suggesting I have a backup project on hand. Your trust in my independence was always appreciated, although occasionally challenging in times of personal scientific panic. It is with your support that I was able to experience scientific research at this depth. Elliot, thank you for listening to me. You push me to be a better (and more scrutinizing) scientist. You are a great teacher. To my beloved undergraduate, Gloria. Thank you for being so much fun and so hardworking. I literally could not have done this without you. You're awesome. Finally, thank you so much to the rest of the Hamdoun lab for being along for the ride.

Thank you to my parents, who have made me feel capable, independent, intelligent, and confident since birth. I'm so lucky to have people like you in my life.

And of course, to Little Joy Coffee Cart, who unofficially sponsored this master's degree. Not just in oat flat whites and raspberry cookies, or Sunday shifts, but through the immense amount of love and support from the other staff and locals. I've never felt part of a community like this one. Thank you.

EPIGRAPH

"I've got information, man. New shit has come to light."

— The Dude

TABLE OF CONTENTS

LIST OF TABLES

LIST OF FIGURES

ABSTRACT OF THE THESIS

Antimicrobial Peptides as a Potential Mechanism for Bacterially Induced Metamorphosis of the Sea Urchin *Lytechinus pictus*

by

Alexis Cody Hargadon

Master of Science in Marine Biology

University of California San Diego, 2023

Professor Amro Hamdoun, Chair

Metamorphosis is a radical morphological and environmental transition from a larval phase to an adult. This process is utilized by ~80% of all animal species and is a particularly common life history strategy among marine invertebrates. It has been well established that across species developmentally competent marine larvae utilize bacterial cues to indicate a suitable habitat conducive to adult survival and reproduction. Despite the high incidence of bacterially

induced metamorphosis, the underlying mechanisms of how animals directly sense these signals remain under-studied, especially in Echinoderms (*e.g*., sea urchins). This study aims to a investigate component of the innate immune system, antimicrobial peptides (AMPs), as a potential candidate for connecting bacterial presence to metamorphosis. To explore AMPs as a player in bacterially induced metamorphosis, I utilized the rapid and synchronously developing sea urchin *Lytechnius pictus.* I first identified a homolog of the Echinoderm specific AMP *Strongylocin 2* in *L. pictus*. I found that *LpStrongylocin 2* (*LpS2l*) is only transcribed in early larvae in the event of bacterial infection. In nascent late-stage larvae, *LpS2l* transcription is upregulated and accumulates within cells in developing adult structures, likely a subtype of blastocoelar cells. The spatiotemporal regulation of *LpS2l* transcription in *L. pictus* larvae suggests a role for AMPs in the development of new structures and recognizing metamorphosis-inducing bacterial cues. Future experiments will be aimed at assessing functional role of *LpS2l* in metamorphosis by disrupting transcription using CRISPR/Cas9 sgRNA guides designed in this study.

INTRODUCTION

Many marine invertebrates utilize a biphasic life cycle transitioning from a planktonic larva to an adult on the benthos. This radical metamorphic transition is a matter of life or death—committing to a favorable environment is paramount for the survival and reproductive success of the adult. Larvae of many species utilize bacterial cues as indicators of a suitable habit (Cavalcanti et al., 2020). While research has accumulated to identify inductive bacterial species for many marine invertebrates, the underlying mechanisms of how animals directly sense these morphogenic signals remain under-studied, especially in Echinoderms (*e.g.*, sea urchins). One growing avenue of research is how elements of the innate immune system may contribute to the recognition of metamorphosis inducing bacterial cues. Antimicrobial peptides (AMPs) are novel candidates for connecting bacteria to developmental events (Lee et al., 2019). A particularly good model system for addressing how AMPs may be involved in metamorphosis is the genetically enabled sea urchin *Lytechinus pictus* which develops quickly and synchronously, able to undergo metamorphosis within 2-3 weeks allowing for greater access to later developmental stages. By taking advantage of this system, I identified a homolog of an Echinoderm specific AMP gene, *Strongylocin 2,* in*L. pictus* (*LpStrongylocin 2)* and evaluated the transcriptional regulation during the larval immune response, development, and metamorphosis. I found that *LpStrongylocin 2* exhibits a pattern of spatiotemporal transcription implicative of a component functioning in the process of metamorphosis.

Bacterially mediated metamorphosis of marine invertebrates

The timing of metamorphosis, an irreversible transition from a larva in the water column to an adult on the benthos, is critical. The larval phase allows for the animal to disperse and explore environments to select the location most promising to promote adult survival and reproduction, and choosing an unsuitable habitat may be deadly. Marine larvae utilize external cues to determine the sustainability of their potential settlement site, many of such cues come from environmental bacteria. Marine biofilms are a consortium of microorganisms which form complex communities on the surface of substrata. The use of microbial biofilms by benthic marine invertebrates dates to the Neoproterozoic era, where filter feeding animals are thought to have preferentially attached to a firm biofilm rather than soft substrata (Hadfield, 2011). The presence of certain bacteria or microbial density is likely indicative of a nontoxic substrate or the growth of a suitable food source for a newly metamorphosed juvenile (Doll et al., 2022).

Animals respond to bacterial cues for settlement and metamorphosis that are secreted from or bound to biofilms, as well as from non-surface bound bacteria. Research has primarily focused on identifying types of inductive bacteria preferred by specific marine invertebrate species (Rischer et al., 2022). For example, strains of *Pseudoalteromonas* stimulate this process in species of corals, Cnidarians, mussels, polychaetes, tube worms, and sea urchins (Rischer et al., 2022). The same is true of *Vibrio* species, found to elicit metamorphosis of polychaetes, corals, sea urchins, oysters, jellyfish, and barnacles (Rischer et al., 2022). Natural products derived from bacteria have also been found have inductive capabilities. One example is the compound tetrabromopyrrole (TBP) produced from *Pseudoalteromona* which stimulates metamorphosis of many coral species (Alker et al., 2023). However, it is unknown whether TBP

is the primary stimulant for corals *in vivo* at ecologically relevant concentrations (Alker et al., 2023).

Many species are relatively nonspecific with the bacterial species or products capable of triggering their metamorphosis. Metamorphosis of the purple urchin *Strongylocentrotus purpuratus* can be initiated in response to water-soluble cues from conspecifics, fleshy and coralline algae, and biofilms (Doll et al., 2022). *S. purpuratus* also appears to have a relatively low specificity for chemical cues able to trigger metamorphosis (Doll et al., 2022). The bacterial species *Pseudoalteromonas luteoviolacea, Shewanella,* and many *Vibrio* species are known metamorphic inducers for *H. erythrogramma* (Huggett et al., 2006).

Despite the large number of marine invertebrate species known to settle and metamorphose in the response to bacterial presence, most of these interactions are understood only at a surface level. The mechanistic basis of recognizing bacterial cues for metamorphosis remain unknown for most species. One direct mechanism behind bacterial-cue signal transduction and metamorphosis has recently been established for the marine tube worm *Hydroides elegans.* Two induction mechanisms have been identified— Metamorphosis-Associated Contractile structures (MACs) and Outer Membrane Vesicles (OMVs) (Freckelton et al., 2017, Shikuma et al., 2014). Once in contact with a dense bacterial biofilm, MACs are deployed from *P. luteoviolacea* bacterium that inject a metamorphosis inducing effector protein called Mif1into the tube worm larvae, immediately stimulating metamorphosis (Shikuma et al., 2014). OMVs of *Cellulophaga lytica* are hypothesized to stimulate metamorphosis through the delivery of an unidentified molecule (Freckelton et al., 2017, Shikuma et al., 2014, Deatherage et al., 2012). Although, this mechanism of stimulus is unique to *H. elegans* and has not yet been

found to occur in other animals. The induction mechanisms of echinoderm metamorphosis are far less elucidated.

Metamorphosis-inducing factors are diverse in their biological and physical properties. Likewise, the mechanisms of sensing and signal transduction utilized to initiate metamorphosis within an animal are just as diverse. Genomic degeneracy, the ability of structurally different elements to yield the same output (Edelman and Gally, 2001), seems particularly important when it comes to critical transitions such as from a larva to a benthic adult. Given the variation in metamorphosis inducing cues within a species it is predicted that multiple mechanisms are at work to ensure a correct signal is recognized. This study proposes that components of the non-self recognition system may serve as an avenue for larvae to recognize bacterial cues.

Larval development and metamorphosis of *Lytechinus pictus*

Sea urchin development begins through external fertilization as adult urchins release gametes into the water column. Fertilized eggs develop through embryogenesis and into free-swimming, filter feeding larvae. Larvae subside on microalgae and diatoms as they are carried throughout the water column (Nesbit et al., 2019). They develop in this form from days to months, depending on the species and influenced by environmental cues. *L. pictus* typically spend 2-3 weeks a larva and progress through 6 developmental stages.

As the larvae grow, a distinct structure called the rudiment develops on the ventral half of the urchin. The rudiment eventually develops into the ventral skeleton and water vascular system of the juvenile sea urchin (Hinegardner, 1975). While the rudiment grows, the larval body serves

as a source of nutrients and protection as it explores potential settlement sites (Hinegardner, 1975). Coinciding with rudiment growth is the formation of external pincher-like structures called pedicellariae. The primary pedicellaria is located on the posterior end of the larva, and two smaller pedicellariae protrude from the right side of the body (Burke, 1980). These small appendages consist of a movable jaw on a flexible stalk (Burke, 1980).

Once the rudiment is fully formed, the larva is competent to undergo metamorphosis. The competent larva becomes negatively buoyant and descends to the sea floor, contacting the substratum with an extended tube foot and opening the larval body (Hinegardner, 1969). If a larva has settled in an unsuitable environment, but has not yet initiated metamorphosis, they have been observed to reverse settlement and resuspend into the water column to search for a better environment (Swanson et al., 2007). In the absence of an appropriate cue, the competent larva may delay settlement and metamorphosis entirely, despite the increased risk of mortality and detrimental carry-over effects on the juvenile and adult animal (Swanson et al.,2007).

Once a larva confirms a location is suitable, several irreversible developmental pathways are initiated. Metamorphosis is rapid and occurs within an hour after initiation. The animal loses larval-specific structures and breaks down the majority of the larval body cells (Doll et al., 2022). Hormonal regulation of programmed cell death (PCD) is the most well understood developmental process behind this event (Wynen et al.,2022). The pedicellariae are shifted to the aboral side of the juvenile and serve as the loci for the formation of the genital plates in the adult test (Burke, 1980). The newly metamorphosed juvenile absorbs a portion of the larval biomass and is decorated by the remanent blanket of cytoplasm on their aboral side for around 24 hours (Hinegardner, 1975). The larval pedicellariae are shed by the juvenile within a week and replaced by structurally identical adult pedicellariae, which are evenly dispersed across the

aboral surface and function in defense and clearance of debris (Hyman, 1955). Before the juvenile urchin begins to feed, internal rearrangements must be completed such as the formation of a complete gut, the anus, teeth, and dorsal skeleton (Hinegardner, 1975). These changes are typically achieved within a week and allow for initial feeding on biofilms until larger jaws are developed and their diet is shifted to kelp (Hinegardner, 1975).

Sea urchin metamorphosis can be induced by a variety of factors. These broadly include gregarious cues from established urchin communities, chemical compounds extracted from preferred algal species (e.g. coralline red algae), neurotransmitters (e.g. dopamine), ions (e.g. potassium), and of particular focus in this study, bacteria (Doll et al., 2022).

Many studies on the factor inducing sea urchin metamorphosis have revealed a distinct effect of bacterial biofilms. Cameron and Hinegardner (1974) detailed the effects of a sterile environment on *L. pictus* and *A. punctulata* settlement and metamorphosis. 62% of larvae were found to undergo metamorphosis when placed in fresh sea water (FSW) in biofilm coated glass dishes, compared to those in sterile glass dishes which yielded no metamorphosis. Notably, when "active" seawater (crude seawater generated through incubation with particulate matter and sediment) was added to biofilm coated plates, the metamorphosis rate rose to 90%. Pearce and Scheibling (1990) also noticed this metamorphic response to biofilms in the species *S. droebachiensus.* Larvae placed in acrylic glass plates that had been incubated in sea water for either 75 days or 40 days, a higher instance of larval metamorphosis was observed in the plates with the older biofilm. Biofilm plates grown in light versus dark conditions showed larvae had an increased percentage of metamorphosis in the light conditioned plates. Interestingly, ATP measurements indicated that both light and dark conditioned plates contained equal bacterial biomass, suggesting a larval preference for specific bacteria rather than its density (Pearce and

Scheibling, 1990). Larvae are likely attracted to bacterial species that become abundant once the basis of biofilm has been established.

Various marine algae are also known to be potent inducers of sea urchin metamorphosis, such as crustose coralline red algae and red algal turf (Pearce and Scheibling,1990). Recently, it has been suggested that the algal cues are instead originating from specific metabolite complexes or bacterial biofilms residing on their surface (Swanson et al., 2007, Dworjanyn and Pirozzi, 2008, Williamson et al., 2000).

How larvae are able recognize specific bacterial cues amidst billions of bacteria in the benthic remains relatively unknown. One approach to identifying non-self recognition systems involved in this transition is by looking within *L. pictus* larval innate immune system.

The larval innate immune system

A small filter feeding larva around 250um in size experiences a constant onslaught of microbes, many of which hold the potential to be pathogenic. This requires a robust system capable of detecting, calibrating, and initiating an appropriate response to the microbial community it encounters. The innate immune system is a complex non-self recognition system built to sense and respond microbes. Sea urchins encode an extraordinary repertoire of expanded innate immune genes, first discovered with the full genome sequencing of the purple urchin (*Strongylocentrotus purpuratu*s) (Sodergren et al., 2006). The most notable expansions were discovered within gene families encoding pattern recognition receptors (PRRs), specifically Toll-like receptors (TLRs), NOD-like receptors (NLRs), and scavenger receptors (SRs) (Buckley and

Rast, 2012). These receptors all function to recognize pathogens either extracellularly (TLRs, SRs) or intracellularly (NLRs). The expansions of these families imply an increased potential capacity for microbial recognition (Buckley and Rast, 2012, Smith et al., 2018).

The larval innate immune system is composed of analogous but different cell types (immunocytes) than that of the adult sea urchin (coelomocytes). Larval immunocytes originate from two distinct waves of mesoderm differentiation during early embryonic development that form pigment cell precursors and blastocoelar precursor cells (Lyons et al., 2011). Pigment cells (PCs) are red granular cells involved in injury response, wound healing, and inflammation. In nascent larvae, PCs are stellate shaped and evenly distributed throughout the larval ectoderm. During an immune response PCs become rounded and migrate towards the site of infection (Ho et al., 2016). These cells can be identified by the transcription of of *polyketide synthase 1* (*PKS1*), which is part of the biochemical pathway that creates echinochrome A. Echinochrome A is responsible for the red color of pigments cells and has demonstrated antimicrobial properties *in vitro* (Hirano, 2016).

There are four morphological subtypes of blastocoelar cells (BCs): filopodial, ovoid, globular, and amoeboid cells. These cells are related by origin but distinguished by morphology and immune capabilities. Filopodial cells have two to five projections and form interconnected syncytial networks throughout the blastocoel, basal surface of the ectoderm, and gut epithelium (Ho et al., 2016). These phagocytic cells engulf foreign objects such as bacteria and express immune effector genes (Ho et al., 2016). One potential marker of filopodial cells is by the transcription of a collagen gene, *col1a(V)chain*. Ovoid cells are phagocytic and only present in the blastocoel following antigen stimulation (Hirano, 2016; Ho et al., 2016). Globular cells are round cells that deploy short filopodial projection to interact with a variety of immune cells and

epithelial cells (Ho et al., 2016). Motile globular cells exhibit surveillance-like behavior throughout the larvae, while sessile globular cells sit within the blastocoelar space of the larval arms and apex (Ho et al., 2016). The fourth type of blastocoelar cell is the amoeboid cell. These 'comma' shaped cells are typically located throughout the blastocoel and able to migrate rapidly to sites of bacterial exposure, as well as interact with the gut epithelium and immune cells, particularly pigment cells (Ho et al., 2016).

Encoded in the sea urchin genome are a suite of immune effector molecules directly involved in pathogen elimination. Of particular interest in this study are antimicrobial peptides (AMPs). AMPs are small peptides with a critical role in the innate immune system in organisms across a wide evolutionary spectrum. Two novel families of AMPs, Centrocins and Strongylocins, were identified from immune cell isolates of the adult green sea urchin *S. droebaciensus* (Li et al., 2008). Centrocins have an intramolecular heterodimeric structure with a heavy chain and a light chain. This family of peptides elicits strong antimicrobial activities against bacteria, fungi, and yeasts (Li et al., 2010). In *S. purpuratus*, Centrocin 1 was localized to blastocoelar cells and stored in granular vesicles (Li et al., 2014). Strongylocins are cationic, defensin like peptides containing a defining cysteine distribution pattern (Li et al., 2008). In adult sea urchins, Strongylocin transcripts have been identified in red spherule cells and phagocytes (Strongylocin 2), and colorless spherule cells/vibratile cells (Strongylocin 1) (Li et al., 2014). While it is known that both Strongylocin 1 and 2 exhibit potent activity against both gram-positive and gram-negative bacteria, their activity and expression in the larval immune response is unknown. The transcriptional regulation of *Strongylocin 2* throughout larval development and metamorphosis is the focus of this study.

Antimicrobial peptide mechanisms of action

AMPs are one of the oldest known immune effector molecules, prevalent through evolution and produced by all life forms. AMPs are extremely diverse and can elicit a variety of specific inhibitory effects against bacteria, fungi, parasites, and viruses, as well as exhibit a broad spectrum of immune activities including antibacterial, antiviral, and antitumor activities (Huan et al., 2020). The vast diversity of antimicrobial families allows for different peptides to be expressed contextually, enabling specific antimicrobial responses depending on the threat. AMPs are traditionally known as potent pathogens killers and most often directly eliminating bacteria via membrane binding and disruption (Wimley, 2010). Certain AMPs utilize intracellular approaches by entering the bacterium without disrupting the membrane and inhibiting central cellular functions (Wimley, 2010). Notably, AMPs are also strong immunomodulators, acting through enhancing bacterial recognition and modulating downstream signaling (Lee et al., 2019).

AMPs bind with immune ligands such as bacterial dsDNA, dsRNA, ssRNA, and LPS to form nanocrystalline structures that amplify host receptor signaling (Lee et al., 2019). These AMP: ligand complexes can increase signaling of bacterial presence by binding to bacterial dsDNA to form a complex nanocrystalline structure able to bind directly to pattern recognition receptors (PRRs), particularly Toll-like receptors (TLRs) (Lee et al., 2019), and lead to activation signal transduction pathways. In the case of AMP- dsDNA, -dsRNA, -ssRNA, these complexes can enter the endosomes of immune cells and bind to complex-specific TLRs (Lee et al., 2019). This engagement with TLRs can lead to modulated pathways including the activation of transcription factors, cytokine production, immune cell chemotaxis, and cellular differentiation and proliferation (Lee et al., 2019). In mammals, AMPs are known to act through this process in the coordinated response of the adaptive system through the activation of T cells

and dendritic cells, stimulation of TLRs, elevation of phagocytosis, the chemoattraction of neutrophils (Zhang et al., 2021). Certain marine invertebrate-derived AMPs have been shown to modulate the human complement system, such as arenicin from the blow lugworm *Arenicola marina* (Umnyakova et al., 2018).

The bacterial recognition and immunomodulatory properties of AMPs present a potential mechanism for larval interpretion bacterial cues and activation developmental processes. To begin validating the hypothesized role of AMPs in metamorphosis, this work investigates the spatiotemporal transcription of the sea urchin specific AMP *Strongylocin 2* throughout development and bacterial exposure.

METHODS

Animal Care and Spawning

Adult *Lytechinus pictus* were initially collected in San Diego, CA, USA and maintained in flowthrough seawater tanks at 18-23°C. Adult animals were spawned by injecting 40uL 0.55M KCl into the peristomal membrane and gently shaken until the observation of gamete release. Eggs were collected from the female continually submerged in FSW, and sperm was pipetted off the male with no contact to water. Larval cultures were maintained in 4-liter beakers at 23°C. Airlines were added at 1 day post fertilization (dpf). Larvae were fed 6,000 cells/mL per day of *Rhodomonas lens* beginning at 2dpf. Cultures were diluted to ~1 larvae/mL at 4dpf and rotated gently with a paddle through metamorphosis.

Strongylocin 2 Identification

A homolog of *Strongylocin 2* was identified *L. pictus* using an NCBI BLASTn search against *SdStrongylocin 2* in Echinodermata (TaxID: 7586) (Altschul et al., 1990). For both phylogenetic tree and protein alignment construction only results with an E value >0 were used from a BLASTp search for LpStrongylocin 2-like (XP_054750701.1) against Echinodermata. A multiple alignment was built using a Genious prime 2022.2.2 alignment (global alignment with free end gaps, Biosum 62) with a 90% consensus threshold for conserved motifs (https://www.geneious.com). The phylogenetic tree was visualized using NCBI distance tree with BLASTp pairwise alignments. Molecular graphics and analyses of immature and mature LpStrongylocin 2 peptide was performed with UCSF ChimeraX, developed by the Resource for Biocomputing, Visualization, and Informatics (San Francisco, CA) (Petterson et al., 2021).

Bacterial Exposure Assay

Vibrio diazotrophicus was cultured as described in Ho et al (2016). Briefly, bacteria were grown to log phase at 15°C and washed 3 times in 0.22 μm FSW and counted in a Petroff–Hauser counting chamber. Prior to exposure, larvae were starved for 12 hours to eliminate transient bacteria within the gut. At 72 hours post fertilization (hpf), 10^7 ml $^{-1}$ *Vibrio* was added to each experimental larval culture only as in Ho et al. (2016) and control cultures were maintained with FSW alone. All cultures were maintained in beakers with 2L FSW. Three experimental replicates were performed using sibling larvae from a unique mate pair for each. Larvae were collected from both unexposed and exposed cultures at 0, 6, 12, and 24 hours post infection (hpi) using a 70um mesh filter and rinsed 3x in FSW prior to fixation.

Sample fixation

Larval and juvenile samples were fixed using a stage-specific optimization protocol from (Choi et al, 2018). Animals were transferred into 1.5 mL Eppendorf tubes and allowed to settle. Samples were rinsed once with 1mL FSW and returned to a volume of 0.5 mL FSW. A deciliation step was included only for 72 hpf larvae, where 50 μL 4.45M NaCl was added to the samples and incubated for 10 minutes. Samples were then rinsed with FSW to a final volume of 1 mL. 72hpf larvae were transferred into a 2 mL cryogenic tube containing a 2 mL solution of 4% PFA, fixation buffer (22.5 mL FSW, 1 mL 5M NaCl, 1.5 mL 1M EPPS), and 1mL FSW. Competent larvae and juveniles were added directly to a 2 mL cryogenic tube containing a 1.8 mL solution containing 100 μL fixation buffer, 400 μL 16% PFA, 300 5M NaCl, 1 mL FSW. All samples were immediately placed on a nutator for 24 hours at 4°C. After incubation, samples were equilibrated to room temperature and 100 μL 1M glycine (1mM EDTA in CMFSW) was

added. Following a 5-minute incubation, samples were rinsed once a solution of 1 mL 1xPBST and 100 µL glycine, twice with 1 mL 1xPBST, and three times with 1 mL 70% EtOH for 10 minutes each. Samples were stored in 1 mL 70% EtOH at -20°C until use as described below.

In situ hybridization chain reaction (HCR)

Probes were selected from a probe library containing HCR probe sets designed for all predicted coding sequences for *L. pictus*. Probe sets were designed using a custom wrapper script to automate insitu_probe_generator (Null, 2019) for the design of all probe-hairpin combinations for all coding sequences. Probes were purchased from Integrated DNA Technologies (IDT; Coralville, Iowa, USA), and amplification hairpins were purchased from Molecular Instruments (El Monte, California, USA). Target sequences and probe-hairpin sequences are available in the supplement (Table S1).

HCR processing steps were adapted from the molecular instruments HCR™ RNA-FISH protocol for whole-mount sea urchin embryos (*Strongylocentrotus purpuratus*), optimized for *L. pictus* larvae ≥72 hpf (Choi et al., 2018). ~100-200 larvae from each fixed sample were rehydrated gradually from 70% EtOH into 0.7mL Eppendorf tubes with 200 µL of 5×SSCT through 3x10 min washes. 5×SSCT was then aspirated and 50 µL of probe hybridization buffer was added and the samples were prehybrized at 37°C for 30 minutes. Probe solution was prepared with 1.5 µL of 1 µM stock probe set to 50 µL of probe hybridization buffer at 37°C. Probe solution was added to the samples and gently mixed to reach a final hybridization volume of 100 µL. Samples were incubated for 24 hours at 37°C.

After incubation, 150 µL of preheated probe wash buffer (37°C) was added to each sample tube and incubated at 37°C for 10 minutes. Excess probes were removed by washing the samples with 200 µL of probe wash buffer for 2x10 minutes and 2x30 minutes remaining at 37°C. Samples were then rinsed into 5xSSCT with 2x10 minute washes at room temperature (RT). 6 pmol per sample of each hairpin (h1 and h2) was snap cooled in separate tubes by heating at 95°C for 90 seconds and allowed to cool in a dark drawer for 30 minutes. Prepared hairpins were then added to room temperature amplification buffer at a ratio of 6 pmol:50 µL. 5×SSCT was removed from the samples and 50 µL of hairpin amplification solution was added and samples were incubated at RT in the dark for 24 hours for optimal amplification.

After amplification incubation, 150 µL of 5×SSCT to each tube and incubated for 5 minutes at RT. Excess hairpins were removed by washing with 200 µL of 5×SSCT for 3x10 minutes followed by 2 x 30 minutes. DAPI nuclear stain was added to the second 30 minute wash at a final concentration of 300µM DAPI 488 stain in 5×SSCT (Invitrogen, Waltham, MA). Competent larvae and juveniles were additionally counterstained with Cell Mask Orange, a plasma membrane stain (Invitrogen, Waltham, MA) by adding 0.01µL of 5mg/mL CMO stock to 1mL of 5×SSCT, and incubating samples in 200µL of the solution for 15 minutes. Samples were rinsed once more in 5×SSCT and stored at 4°C protected from light before imaging.

Confocal microscopy

Prior to confocal imaging, ~75 larvae were transferred into 80% glycerol using a stepwise rinse of 70/30 5xSSCT:100% Glycerol, 50/50, and 20/80. Larvae were gently plated into wells of a Cellvis glass bottom 384-well plate (Mountain View, California, USA) at a density of ~30 larvae per well. Imaging was performed on a Molecular Devices ImageXpress HT.ai (San Jose,

California, USA) using a 20X Nikon Plan Apochromatic objective. Laser channels used in this study include 750, 647, 594, 488 and 405 nm, along with the appropriate emission filters. All 72-96hpf larvae were imaged in 3µm Z-stacks with a 100 ms exposure time and 50% laser power. Competent larvae were imaged using a Leica TCS SP8 X White Light Laser Confocal Microscope Image with identical parameters. Image processing was conducted using ImageJ to create 2D projections of the appropriate range of stacks, adjustments to brightness and contrast, scale bar generation (pixel ratio of 3.416 pixels/1um) and cropping of single larvae (Schindelin et al. 2019). 3D renderings were generated with Imaris (https://imaris.oxinst.com/). Negative controls for non-specific signal deriving from reagent chemistry include larvae which have been processed without probes (Figure S1).

Developmental transcriptome analysis

Lytechinus pictus developmental transcriptome analysis was generated from RNA-seq data accessible on Echinobase (Arshinoff et al., 2022) and NCBI (PRJNA952574). Transcripts per million were averaged for each gene and plotted using R studio 2021.09.0 (http://www.rstudio.com/).

gDNA Primer and probe design

ChopChop v.2 (https://chopchop.cbu.uib.no) (Labun et al., 2016) was used to design guide RNAs (gRNAs) against *LpS2l*. Guides were designed targeting Exons 1 and 2. Synthetic sgRNAs (Ex1-93, GTGAAGCCATTGTTTGAGACAGG; Ex2+24, CCAATGCGAGAGAAGAATCTTGG) were ordered from Synthego (Redwood City, CA). 1.5 nmol of each sgRNA was resuspended in 15 µl nuclease-free water and stored in aliquots at

−80°C. Embryonic microinjections of one wild type mate pair were performed using a solution of 150ng/ul of each sgRNA and 750ng/uL of Cas9 mRNA to create mutations at both target sites. Rhodamine B (RhoB; Thermo Scientific Chemicals) was co-injected at a concentration of X as a positive injection control. Embryos were screened for RhoB red fluorescence on an Epi-Fluorescence Stereoscope (Leica M165 FC) and non-fluorescent embryos were removed.

Genotyping/Mutation validation

Genotyping was conducted on individual injected larvae and wild type larvae from the same mate pair at 7 dpf to validate guides. Genomic DNA was extracted using the Qiagen QIAamp DNA micro kit according to the manufacturers' instructions. Primers flanking exon 1 (Amp_Int0_F2, CCACTTTCAACCATTCTCAACTATTCCA; Amp_Int1_R2, GGGCGGAGTGGGAGAAAGAAAATAGAAG) and exon 2 (AMP1_Int2_F1, AAGTCCGGTATACTACTATGCAATGTTTTC; LpAMP1_Ex2_89R, ACACGTCATTTTACCTGTTGTTTGAC) were used separately to amplify regions of Exons 1 and 2. Following initial amplification, nested primers were used for both exon 1 (AMP1-Ex1_8Fm13, TAGGTGACACTATAGTGTAAAACGACGGCCAGTTCGTTCTTTCGTTTCTT CTGTAGCATA; AMP1_Ex1R1m13, ACGACTCACTATAGGGCAGGAAACAGCTATGAC AATATACATGCAGGCCTACTTACCA) and exon 2 (AMP1_Int2_1Fm13, TAGGTGACACT ATAGTGTAAAACGACGGCCAGTAAGTCCGGTATACTACTATGCAATGTT; AMP1_Ex2_89Rm13, AATACGACTCACTATAGGGCAGGAAACAGCTATGACACAC GTCATTTTACCTGTTGTTTG) containing m13 overhangs to allow for full exon sequencing. Secondary PCR samples were cleaned using the Qiagen QIAquick PCR & Gel Cleanup Kit according to the manufacturers' instructions and sequenced through Eurofins Genomics

(Louisville, KY). Indels generated were initially visualized using SnapGene® software (from Dotmatics; available at snapgene.com) and further confirmed using the Synthego ICE tool (https://ice.synthego.com/#/) to identify indel percentages within a mosaic individual.

Metamorphosis Assays

Culturing of CRISPR/Cas9 dual guide injected and wild type larvae was conducted as previously described (Fleming, 2021; Vyas et al., 2022). Survivorship and larval morphology were assessed by eye on a Leica M165 FC every 2 days leading up to metamorphosis. Larvae were allowed to settle and metamorphose naturally within the beaker. Animals were scored as metamorphosed after spines were fully visible from beneath the larval body. The number of fully metamorphosed larvae was recorded each day starting with the first instance of metamorphosis up until 50 dpf.

RESULTS

I. Identification of the antimicrobial peptide *Strongylocin2* in *Lytechinus pictus.*

Because antimicrobial peptides amplify innate immune signaling, I sought to identify homologs of echinoderm specific AMPs in *Lytechinus pictus*. Two unique families, Centrocins and Strongylocins, have been previously identified and characterized in the sea urchin species *S. droebaciensus, S. purpuratus,* and *E. esculentus*, but have yet to be identified in *L. pictus*. An NCBI BLASTn search within Echinodermata against AMPs within these families (*Centrocin 1, Centrocin 2, Strongylocin 1*, and *Strongylocin 2* from *Strongylocentrotus droebaciensus*) revealed only one homolog to be present in the *L. pictus* genome, which has been termed *LpStrongylocin 2* (Figure 1A).

Genomic sequencing of *L. pictus* larvae confirmed the characteristically short 4-exon structure consistent with that of *SdStrongylocin 2*. The nucleic acid coding sequence spans 4,271 base pairs (bp) with 4 small exon lengths in comparison to the 3 introns. The 4 exons are 97, 101, 79, and 17 bp respectively, with the fourth exon containing a long UTR region (Figure 2C). The short peptide length is consistent across antimicrobial peptides (Mahlapuu et al., 2016).

Protein alignments revealed a significant conservation of residues across echinoids, including the 6-cysteine (Figure 1A, B). The Strongylocin family, including LpStrongylocin 2, protein sequence contains 6 cysteines with a unique distribution pattern of where cysteines four and five are adjacent to each other (Li et al., 2008). These peptides are categorized as a subfamily of defensins, one of the most diverse groups of AMPs within invertebrates that vary in both genomic organization and sequence identity but grouped by their high number cysteine residues (Li et al., 2008). The location of these residues is responsible for the disulfide bridges of the peptide which stabilize the structure (Huan et al., 2020). LpStrongylocin 2 contains 96aa,

with the signal peptide beginning at the 5' end containing 22aa, followed by the 18aa prosequence and the 56aa mature peptide coding region (Figure 1C'). Despite the characteristic diversity of sequences within each AMP, even between species, the conserved preprosequence within the precursor molecules remains categorizable (Zasloff, 2002). The immature peptide is synthesized and stored in this inactive form until it is post-translationally modified and the preprosequence is removed, altering the peptide conformation and charge (Figure 1D). Once these modifications have been made the positively charged regions are exposed and the mature peptide is able to exhibit antimicrobial activity (Figure 1D').

Predicted secondary structures were generated with ChimeraX (San Francisco, CA) (Petterson et al., 2021), confirming both the immature and mature LpS2l peptide contain the defense-like signature beta sheet-alpha helix structure (Figure 1D, D'). This structure is formed by 3 disulfide bonds that influence antimicrobial activity and protect against degradation during biosynthesis thorough the stabilization of its molecular structure (Li et al., 2010).

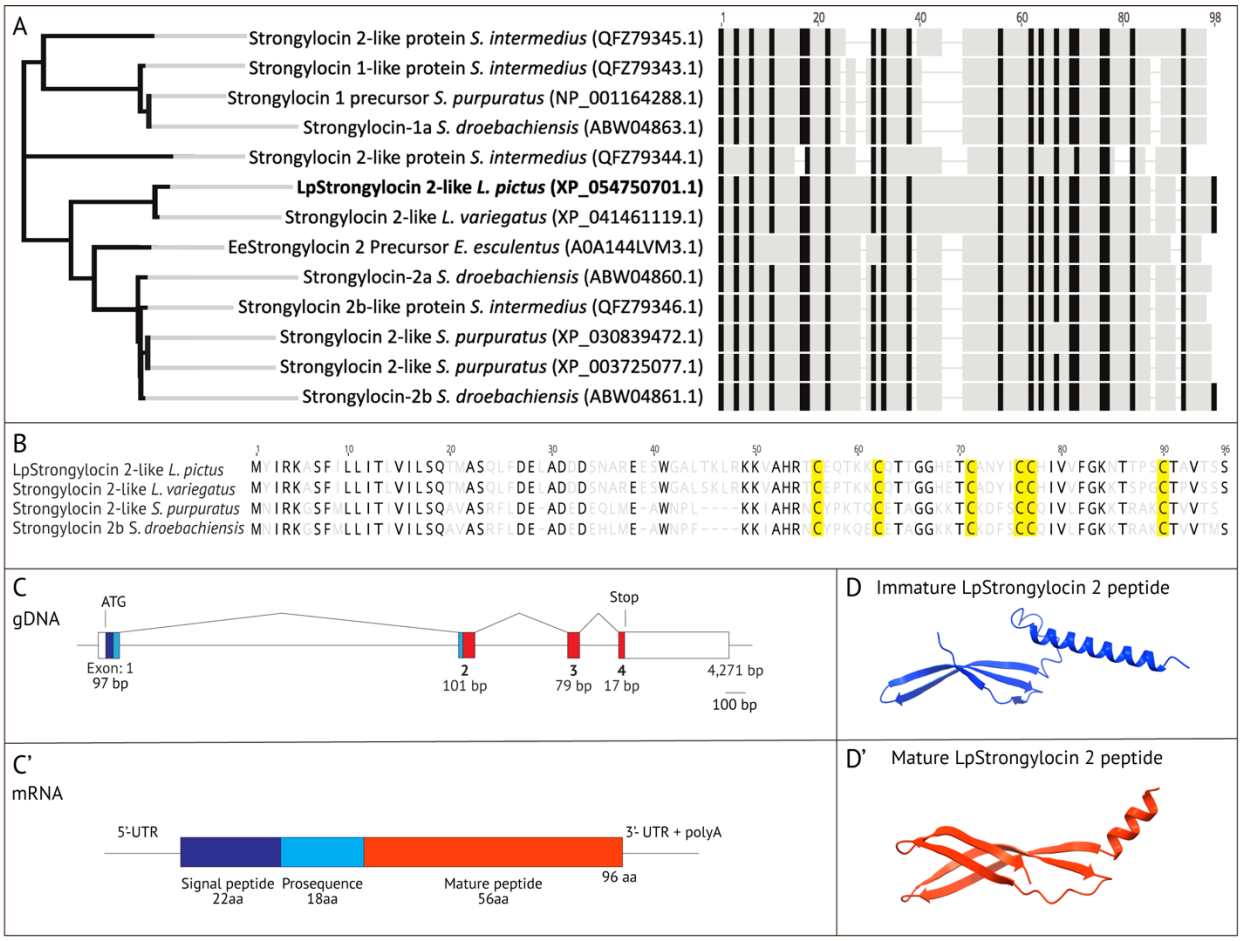

Figure 1. Gene model and protein topology of *LpStrongylocin 2* in *Lytechnius pictus*. **(A)** Identification of LpStrongylocin 2 in *Lytechinus pictus*. Black bars of the protein sequence alignment indicate a 90% consensus threshold among query sequences. **(B)** Amino acid sequence alignment of Strongylocin 2 homologs in *L. pictus, L. variegatus, S. purpuratus,* and *S. drobachiensus*. The signature 6 cysteine pattern of Stronglyocin 2 is highlighted in yellow. **(C)** The genomic DNA sequence of *LpStrongylocin 2* contains 4 exons and 3 introns. Colored portions of exons correspond with the encoded signal peptide (dark blue), prosequence (light blue), and mature peptide sequence (red) shown in the mRNA model **(C')**. **(C')** The mRNA of *LpS2l* consists of a signal peptide, prosequence, and mature peptide sequence. **(D,D')** Predicted protein structure of the immature and mature LpS2l peptide.

II. *LpStrongylocin 2* is transcribed by epithelial cells in response to bacterial challenge.

Antimicrobial peptide expression is regulated in many organisms. It is often synthesized and released from epithelial cells or immune cells upon stimulation (Huttner and Berins, 1999, Blyth et al., 2022). While the transcriptional response and antimicrobial capabilities of Strongylocin 2 have been confirmed *in vitro*, the inducibility or activity of Strongylocin 2 within live sea urchin larvae was previously unknown. To investigate the responsiveness of *LpStrongylocin 2* to bacteria, I used HCR RNA-FISH to localize transcript accumulation within 3 day old larvae over the course of a 24-hour immune challenge to the marine bacterium *Vibrio diazotrophicus*.

Only a minority of 3dpf uninfected larvae displayed *LpS2l* signal, which was observed near the midgut (Table 1A, Figure 2A, E). After 6 hours of exposure to *Vibrio, LpS2l* transcript signal was observed within the gut, increasing by hour 12 (Figure 2 B, C). The signal localization suggests *LpS2l* is being expressed by gut epithelial cells, consistent with AMP responses of other marine invertebrates to bacterial challenges (Lv et al., 2020, Mitta et al., 1999). About half of the exposed larvae at 24 hours post infection were observed to have ~1-2 cells with *LpS2l* transcript accumulation, often located near the foregut (Figure 2D). Variation in responsiveness was evident both within and between mate pairs (Table 1). Mate pair 1 displayed a robust response, whereas mate pairs 2 and 3 did not display a response of similar magnitude (Table 1B- D). Throughout the 24-hour period an increase in the number of unexposed larvae with *LpS2l*+ cells were observed (Table 1E-G). This is a probable effect of the starvation period and subsequent exposure to decreasing bacterial levels, and *LpS2l* transcripts are likely accumulating within immune cells throughout the larva rather than being activated more rapidly. Most observed cells containing *LpS2l* transcript were present near the foregut or by the larval

head (Figure 2D, F-H). Occasionally *LpS2l*+ cells were observed on the apex of the arms or by the shoulder. These areas are typically exposed to higher concentrations of microbes, suggesting *LpS2l* is transcribed in surveillance/motile cells able to migrate throughout larvae at this stage of development, however life imaging is necessary to confirm this.

Figure 2. *LpStrongylocin 2* is transcribed in response to bacterial challenge in early-stage larvae. (A-D). (A,E). *LpS2l* signal is present in a small subset of 72hpf larvae within cells near the foregut. **(B,C)** Cells within the midgut of exposed larvae have *LpS2l* transcripts at 6hpi, increasing in magnitude by 12 hpi. **(D)** At 24hpi, ~1-2 *LpS2l* + cells are observed near foregut or throughout the body. **(F-H)** Transcript localization patterns of *LpS2l* in unexposed larvae remained consistent throughout the trial. Box insets highlight the localization of *LpS2l* + cells both with DAPI overlay **(A'-D', E'-H')** and only the fluorescence channel (746mn) **(A''-D'', E"-H")**. (A-H) Scale bar= 50µm. (A'-H', A"-H") Scale bar = 25µm.

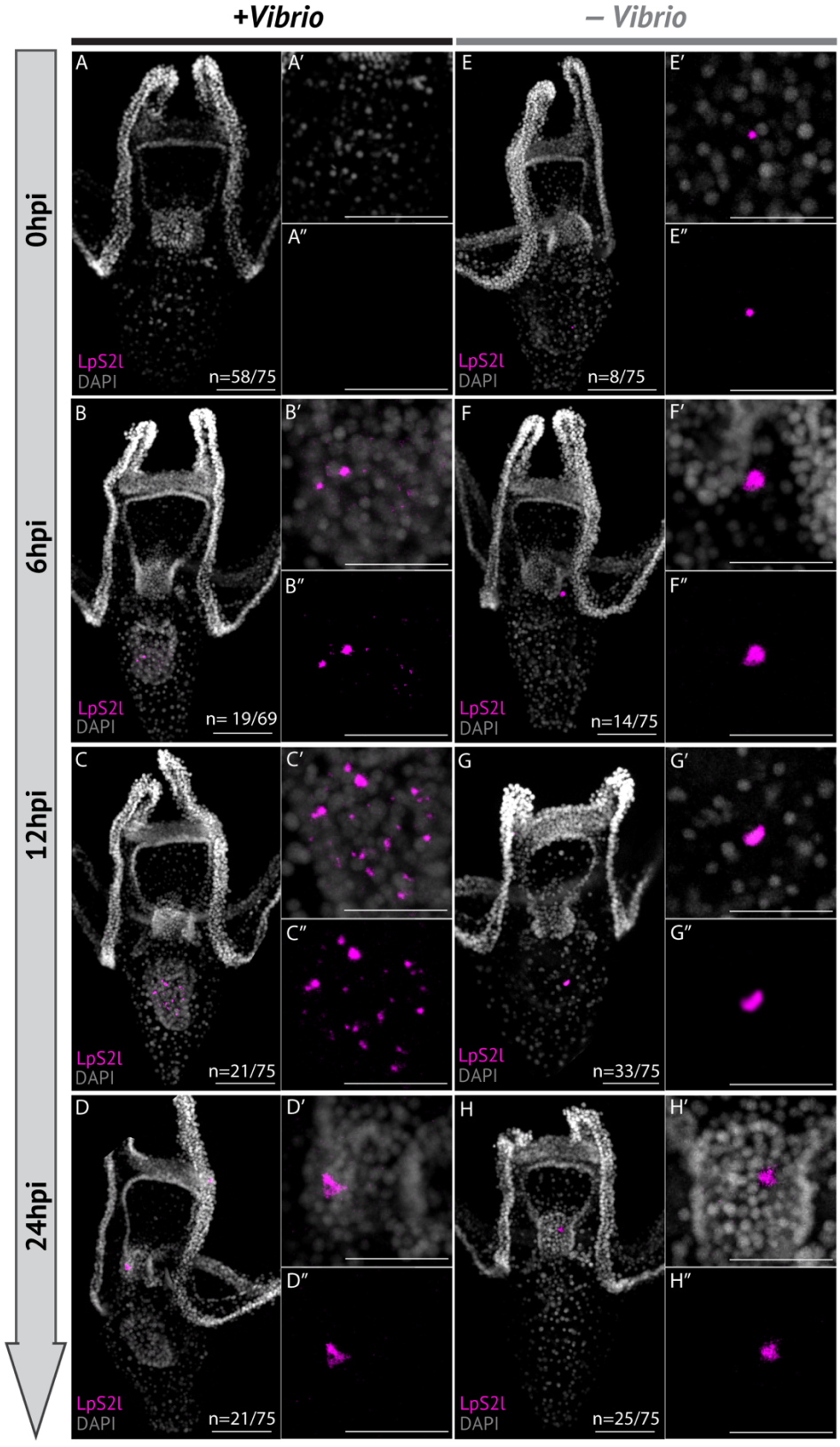
+Vibrio
– Vibrio
0hpi
6hpi
12hpi
24hpi
A
A′
A″
E
E′
E″
B
B′
B″
F
F′
F″
C
C′
C″
G
G′
G″
D
D′
D″
H
H′
H″
LpS2l
DAPI
n=58/75
n=8/75
n= 19/69
n=14/75
n=21/75
n=33/75
n=21/75
n=25/75

Table 1. HCR RNA-FISH reveals variation in larval *LpS2l* transcriptional response during bacterial exposure. Rows labeled MP 1, 2, and 3 indicate the localization patterns at each timepoint within the corresponding mate pair (MP). +*Vibrio* (black) tables list observations from exposed cultures. -*Vibrio* (grey) tables list observations from unexposed cultures. **(A)** The majority of immunoquiescent larvae collected prior to exposure did not show LpS2l transcriptional signal. Occasional LpS2l signal was observed within cells throughout the larval body. (**B, B'**) Mate pair 1 was found to have a more larvae with *LpS2l* gut transcription compared to MP 2 and 3. Transcription within the gut of unexposed larvae was not observed. **(C, C')** Signal was more frequently present within the gut of exposed larvae at 12 hpi, whereas transcription in more dispersed cells within the larva was observed when unexposed. **(D, D')** The distribution of *LpS2l* localization patterns is similar between exposed and unexposed larvae at 24hpi.

A 0hpi

	No signal	Signal within gut	1-2 cells	N=
MP 1	17	3	5	25
MP 2	24	1	0	25
MP 3	17	4	4	25

B 6hpi + *Vibrio*

	No signal	Signal within gut	1-2 cells	N=
MP 1	8	17	0	25
MP 2	19	1	2	22
MP 3	17	1	4	22

B' 6hpi - *Vibrio*

	No signal	Signal within gut	1-2 cells	N=
MP 1	11	1	3	15
MP 2	14	2	9	25
MP 3	12	6	2	25

C 12hpi + *Vibrio*

	No signal	Signal within gut	1-2 cells	N=
MP 1	6	18	1	25
MP 2	23	1	1	25
MP 3	20	2	3	25

C' 12hpi - *Vibrio*

	No signal	Signal within gut	1-2 cells	N=
MP 1	11	2	12	25
MP 2	15	0	10	25
MP 3	12	2	11	25

D 24hpi + *Vibrio*

	No signal	Signal within gut	1-2 cells	N=
MP 1	13	1	11	25
MP 2	21	0	4	25
MP 3	19	0	6	25

D' 24hpi - *Vibrio*

	No signal	Signal within gut	1-2 cells	N=
MP 1	15	2	8	25
MP 2	16	0	9	25
MP 3	7	0	8	15

III. *LpStrongylocin 2* transcription is upregulated immediately prior to metamorphosis.

Given the observed response of *LpS2l* to bacterial exposure, I next sought to characterize its transcriptional regulation leading up to the time when bacterial cues are known to initiate metamorphosis (Figure 3). In nascent larvae, *LpS2l* is not transcribed at detectable levels until the early larval stage, where transcription is likely initiated with the onset of feeding and thus increased exposure to natural/dietary sources of bacteria. A sharp increase in *LpS2l* transcription at the medium and large rudiment stage coincides with the achievement of metamorphic competency, around 2-3 weeks post fertilization. To confirm this increase is not a result of exposure to a denser bacterial population, transcriptional levels of other immune gene markers were compared (Figure 3). Interleukin 17D (*IL17D*) is a cytokine involved in the activation and mediation of the immune response, only activated during an active infection (Buckley et al., 2017). This gene is not transcribed at a detectable level throughout larval development, indicating the larvae sampled remained immunoquiescent. *PKS1* and *srcr142*, expressed in pigment cells, exhibit an increase in transcription at the late gastrula stage then remain at a lower level throughout development. *LpS2l* remains transcribed at this higher level at the juvenile stage 24 hours post metamorphosis. It should be noted that at this time the newly metamorphosed juvenile is still partially covered by the decaying larval body, which may be contributing transcripts. Strongylocin 2 is present in the coelomocytes of other sea urchin species (Li et al., 2008, Li et al., 2010, Solstad et al., 2016), which are likely also a source of *LpS2l* transcripts at this stage.

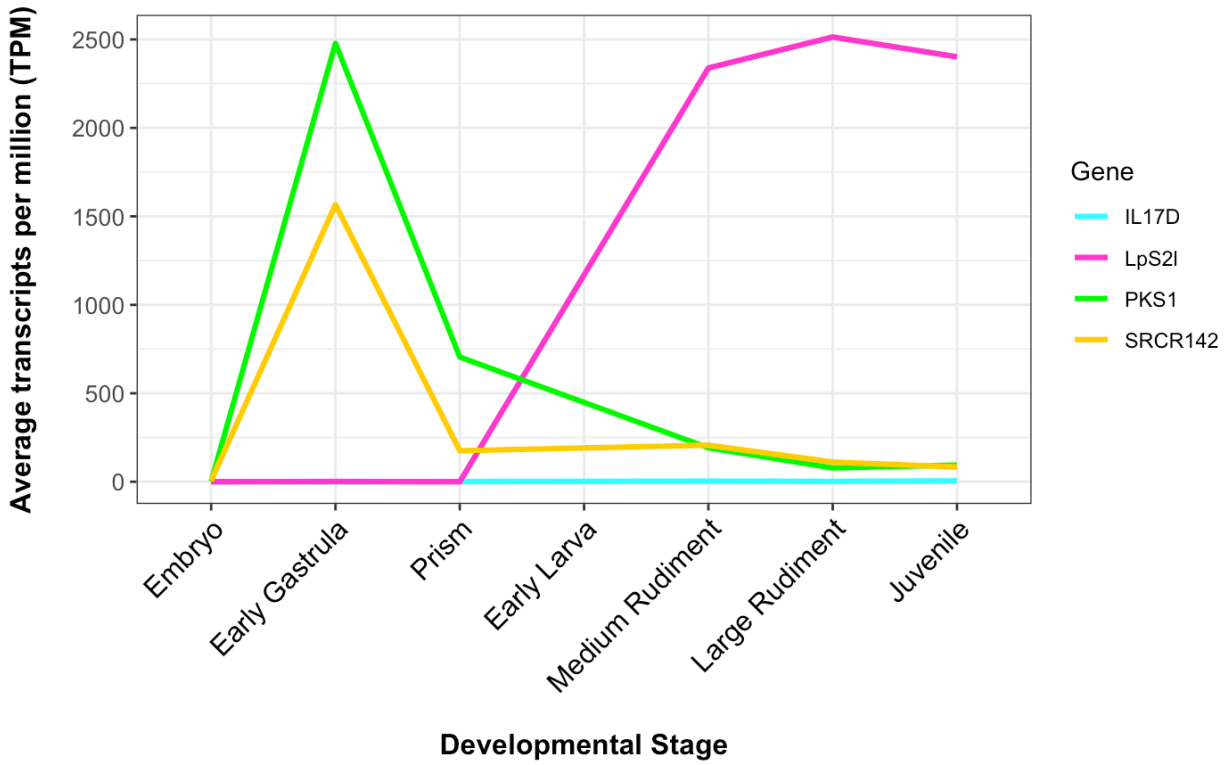

Figure 3. ***LpStrongylocin 2*** **transcription is upregulated prior to metamorphosis.** Average transcription levels (TPM) by developmental stage of target immune genes, *IL17D* (cyan), *LpS2l* (yellow), *PKS1* (green) and *srcr142* (magenta). Developmental stages are listed from left to right by sampled stages. Early larvae represent the four arm pluteus stage. Medium and large rudiment represent stage 5 and stage 6 larvae, respectively. The juvenile stage was sampled 24 hours post metamorphosis. Average transcripts per million reads were generated from the Echinobase database of the *Lytechinus pictus* developmental transcriptome.

IV. *LpStrongylocin 2* is likely transcribed by ameboid cells.

Larval immunocyte transcription of Strongylocins was previously unknown. Based on the previous finding that Strongylocin 2 is present in red spherule cells of adult *S. purpuratus* (Li et al., 2010)*,* I hypothesized *LpS2l* transcripts would be localized to pigment cells in the larvae. Using HCR RNA-FISH to co-staining *PKS1,* a molecular marker of pigment cells, and *LpS2l,* I found *LpS2l* transcription is not colocalized with *PKS1* and instead was observed in comma shaped cells often directly interacting with pigment cells near the rudiment (Figure 4A, B). Considering that Strongylocins are found in larvae of other species to be transcribed by immune cells (Li et al., 2010) it is likely being transcribed by subtype of blastocoelar cells. In *S. purpuratus* globular and ameboid cells have been shown to engage with pigment cells as a form of cellular communication (Ho et al., 2016). This interaction is visible between the pigment cells and *LpS2l*+ cells in *L. pictus* larvae, suggesting the observed cells are either globular or ameboid, The morphology of *LpS2l*+ cells (Figure 5C') resembles ameboid cells (comma-shaped) rather than globular cells (round).

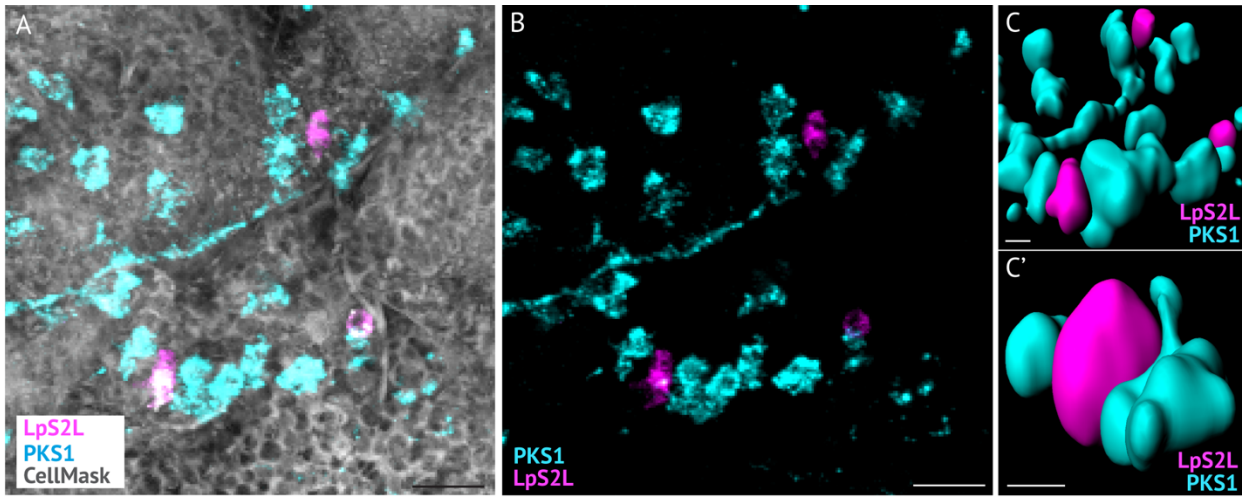

Figure 4. Cells with accumulated *LpStronglyocin 2* transcripts interact with pigment cells. **(A,B)** HCR RNA-FISH image of *LpS2l*+ cells (magenta) interacting with pigment cells (marked by *PKS1,* cyan). **(C,C')** 3D rendering of *LpS2l*+ cells nestled between pigment cells generated with Imaris 3D image analysis software (https://imaris.oxinst.com/). Scale bars= 10µm**.**

To investigate the possibility that *LpS2l* is transcribed in a different or additional blastocoelar subtype, I co-stained competent larvae for *LpS2l* and *col1a(V)chain,* a hypothesized filopodial cell marker. No colocalization was observed between *LpS2l*+ and *col1a(V)chain*+ cells, although these cells were often localized near the same regions (Figure 5 A-C). The morphology and localization pattern shown in *L. pictus* (Figure 5 C') supports the conclusion that *LpS2l* is being actively transcribed or stored in amoeboid cells, however there are currently no known genetic markers for this cell type.

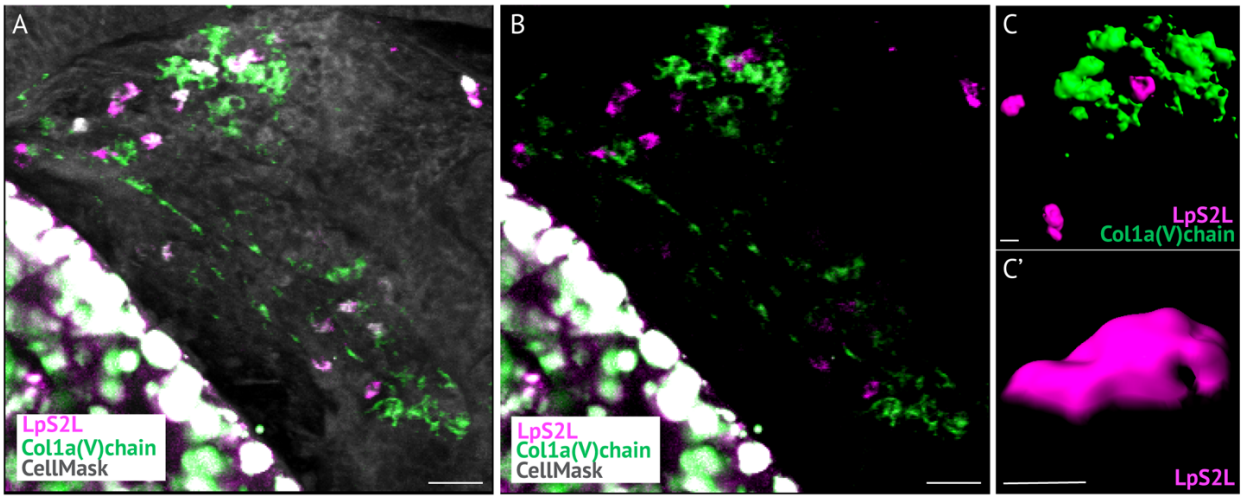

Figure 5. Cells with accumulated *LpStronglyocin 2* transcripts are found near potential filopodial cells. (A,B) HCR-RNA FISH co-staining of *LpS2l* and *col1a(V)chain* shows these genes are not transcribed within the same cells. Fluorescence within the gut in the bottom left corner is autofluorescence and present in negative controls. (C**)** Imaris 3D rendering of *LpS2l:Col1a(V)chain* cellular interactions (https://imaris.oxinst.com/). **C')** 3D rendering of *LpS2l+ cell.* Scale bars= 10µm.

V. Cells with *LpS2l* transcripts are present within developing structures.

The localization of Strongylocin transcripts in larvae of any urchin species has not been previously reported. HCR RNA-FISH was used to determine where *LpS2l* is transcribed immediately prior to metamorphosis. It was hypothesized that in competent larvae, around -3 weeks old, *LpS2l* transcripts would be present in cells within the gap junction between the gut and the rudiment. Accumulated *LpS2l* transcriptional signal was instead observed in cells within the tissue of the developing rudiment (Figure 6).

Surprisingly, signal was also evident in cells located within the epidermal tissue of both the primary pedicellaria and two right pedicellaria (Figure 7). Cells with *LpS2l* transcripts are localized to the epidermal tissue at the base and along the stalk of the pedicellariae, and notably absent from the skeletal jaw. The localization of *LpS2l* transcripts suggests tissue resident immune cells could be a player in the regulation and development of adult structures.

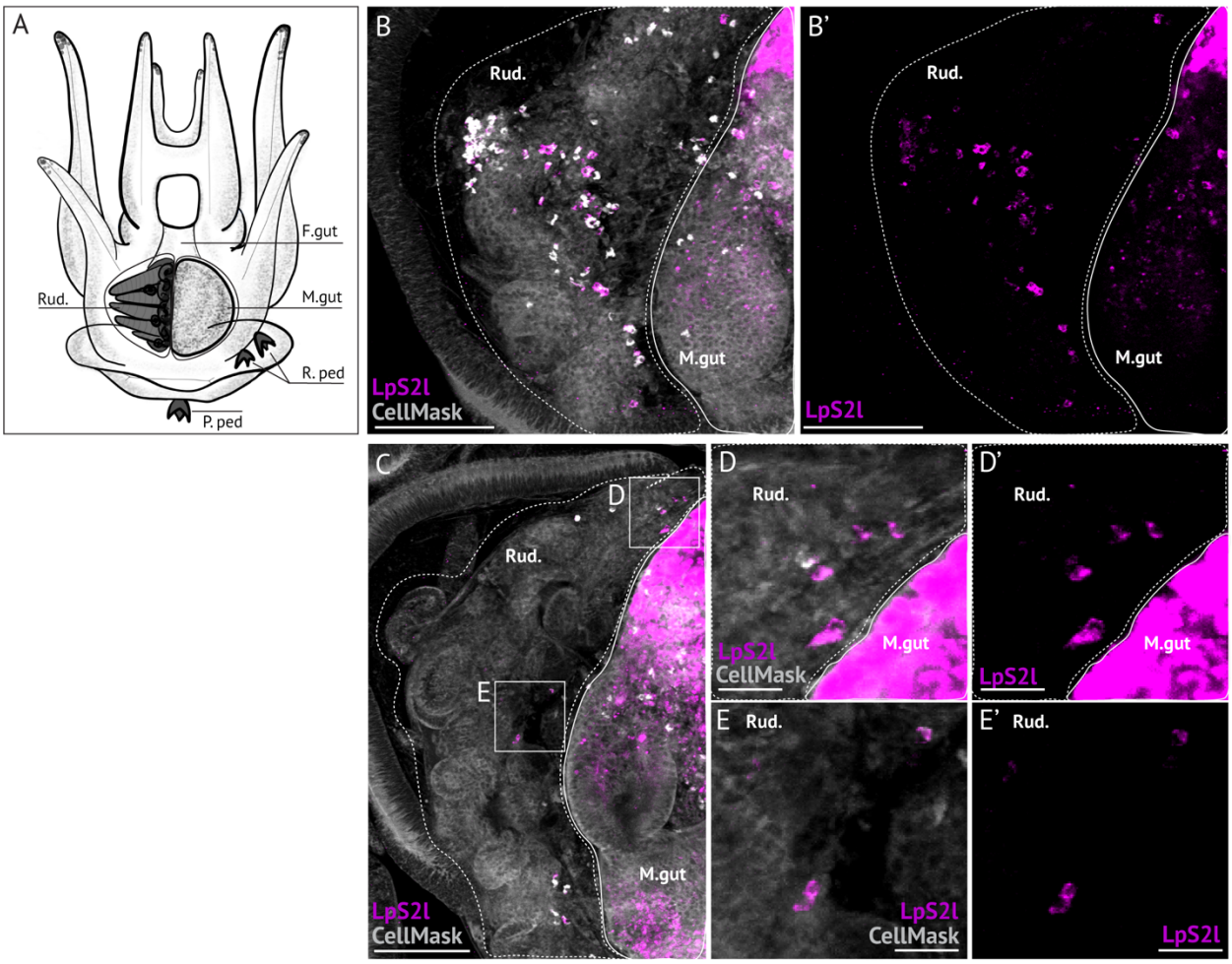

Figure 6. Rudiment tissue contains cells with accumulated *LpStrongylocin 2* transcripts. (A) Graphic of competent larval morphology. Rud. = rudiment, F. gut= foregut, M.gut = midgut, R. ped= right pedicellariae, P.ped= primary pedicellaria. **(B,B')** Z-stack of competent larval rudiment and midgut region. *LpS2l*+ cells (magenta) within the rudiment tissue. **(C)** Z-slice of the same larva as in (B,B'). *LpS2l*+ cells are present in the top left corner at the edge of the rudiment, as well as within the rudiment tissue in the center **(D-E')** Insets of (C) with Cell Mask overlay **(**D,E**)** and without **(**D',E'**)**. Dashed white lines outline the rudiment structure, and solid white lines outline the midgut. Fluorescence in the upper right corner of the gut is autofluorescence. (B-C) Scale bar = 10µm, (D-E') Scale bar= 10µm.

Figure 7. Cells with *LpS2l* transcripts are present within the epidermal tissue of pedicellariae. (A) Graphic of pedicellaria morphology. Jaw = Jaw of pedicellaria head, Mus = muscle of jaw, Stalk = stalk, ep. = epidermal cells, My. = mesenchymal cells, Sk = skeletal tissue. Region under black lines above mesenchymal bulb is the larval hood. **(B,B')** Whole view of the primary pedicellaria. *LpS2l* transcripts (magenta) are often present in cells visibly white from Cell Mask membrane stain. **(C,C')** ∫*LpS2l*+ cells on the epidermal tissue of the stalk. **(D,D')** *LpS2l*+ cells are associated with three larval pedicellaria. Signal is evident on the epidermis of the primary pedicellaria stalk. Epidermal cells are outlined in the solid white line, and mesenchymal cells are outlines in dashed white lines. Scale bar= 50µm.

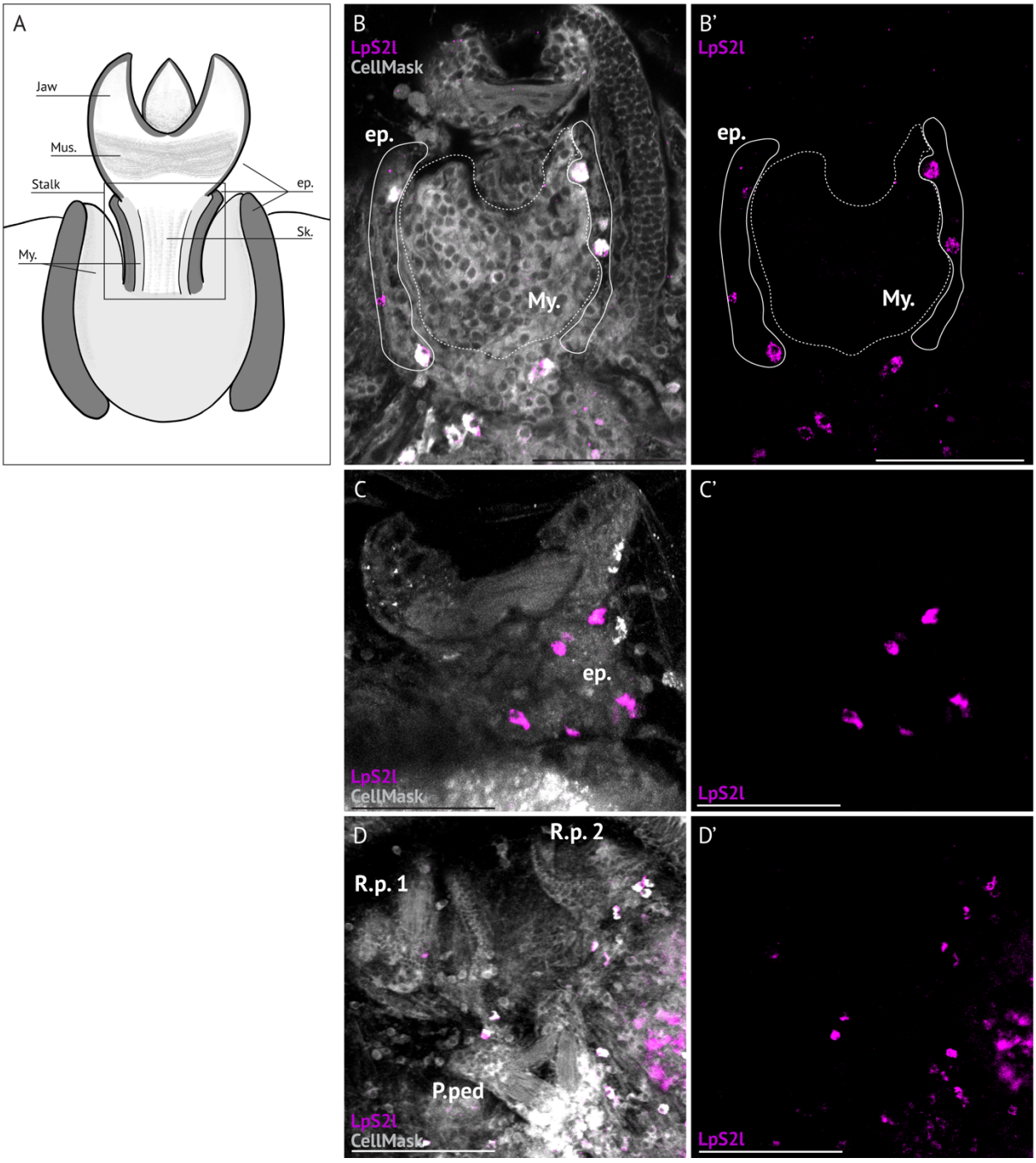
A
Jaw
Mus.
Stalk
ep.
Sk.
My.
B
LpS2l
CellMask
ep.
My.
B'
LpS2l
ep.
My.
C
ep.
LpS2l
CellMask
C'
LpS2l
D
R.p. 2
R.p. 1
P.ped
LpS2l
CellMask
D'
LpS2l

Immediately following metamorphosis, *LpS2l* transcript signal is present on both the aboral and oral surface of the juvenile (Figure 8). The aboral signal is likely within the cytoplasmic remains of the larval tissue. Fewer cells on the oral side are observed to be transcribing *LpS2l* compared to the aboral. Signal is localized to the oral tissue in a pentaradial distribution. No signal was visible on either side of 1 week old juveniles. Visualization of internal cellular mRNA using HCR RNA-FISH is limited by the juvenile tissue and skeleton. However, based on RNA-seq transcriptional data (Figure 3) and previous work done in *S. purpuratus* (Li et al., 2010) it is expected that adult coelomocytes are additionally transcribing *LpS2l* at the juvenile stage.

Figure 8. *LpStronglyocin 2* transcripts are visible on the ectoderm of newly metamorphosed juveniles. (A,A') Aboral view of a juvenile 6 hours post metamorphosis (hpm). Cytoplasm covering the aboral side of the juvenile shows *LpS2l* signal evenly distributed across the outer ring of the body. **(B, B'')** Signal is present on the oral side of the juvenile 6hpm. **(C-D').** No signal is observed on either the aboral or oral side of one week old juveniles. Scale bar = 50μm.

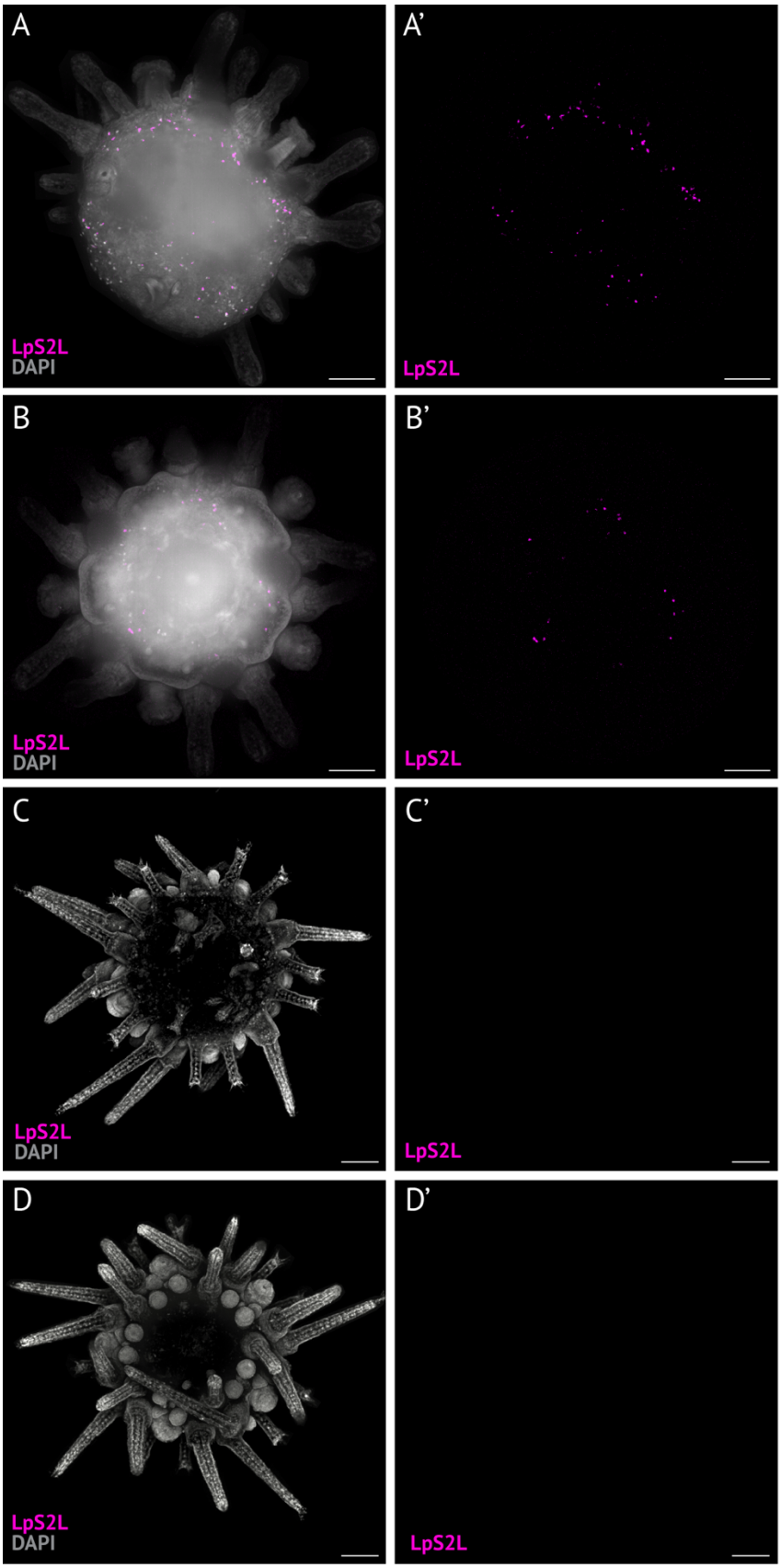
A
LpS2L
DAPI
A'
LpS2L
B
LpS2L
DAPI
B'
LpS2L
C
LpS2L
DAPI
C'
LpS2L
D
LpS2L
DAPI
D'
LpS2L

VI. Generation of CRISPR/Cas9 sgRNAs for *LpS2l* knockdown.

To begin assessing the functional role of LpS2l in the initiation of metamorphosis, CRISPR/Cas 9 gRNAs were generated and validated to functionally disrupt *LpS2l* in *L. pictus*. Two guide RNAs designed to target exon 1 (Exon1- 93) and exon 2 (Exon2+24) were microinjected into *L. pictus* embryos (Figure 9A). The injection success was confirmed initially through visualization of the fluorescent control marker RhoB. The indels generated were confirmed with sequencing the genomic DNA sequencing of individual larvae. Both guides yielded mosaic indels of single nucleotide polymorphisms or short deletions surrounding the target cut sites (Figure 9B, C). No large deletions were detected in the larvae sampled.

The survivorship of *LpS2l*-perturbed larvae and wild type controls remained similar throughout development. Both cultures experienced a decline in survivorship around day 7-10 (Figure 10A), but this observation was not considered abnormal at this particularly sensitive stage of development and often occurs in laboratory cultures. The developmental rate of the mate pair tested was notably longer (~3-4 weeks) than is typical for *L. pictus* (~2-3 weeks). This could be an artifact of the mate pair, culturing conditions, food availability, or season. Larvae from both groups attained metamorphic competency synchronously at around 4 weeks, suggesting an external cause for the delay in development. Despite being metamorphically competent, *LpS2l*-perturbed larvae demonstrated delayed initiation of metamorphosis by around 5 days compared to the sibling-matched wild type controls (Figure 10B). Of the larvae that were able to complete metamorphosis, only 30% of the *LpS2l*-disrupted animals metamorphosed compared to 66% of WT. To further validate these results, additional trial replicates are required for at least two mate pairs.

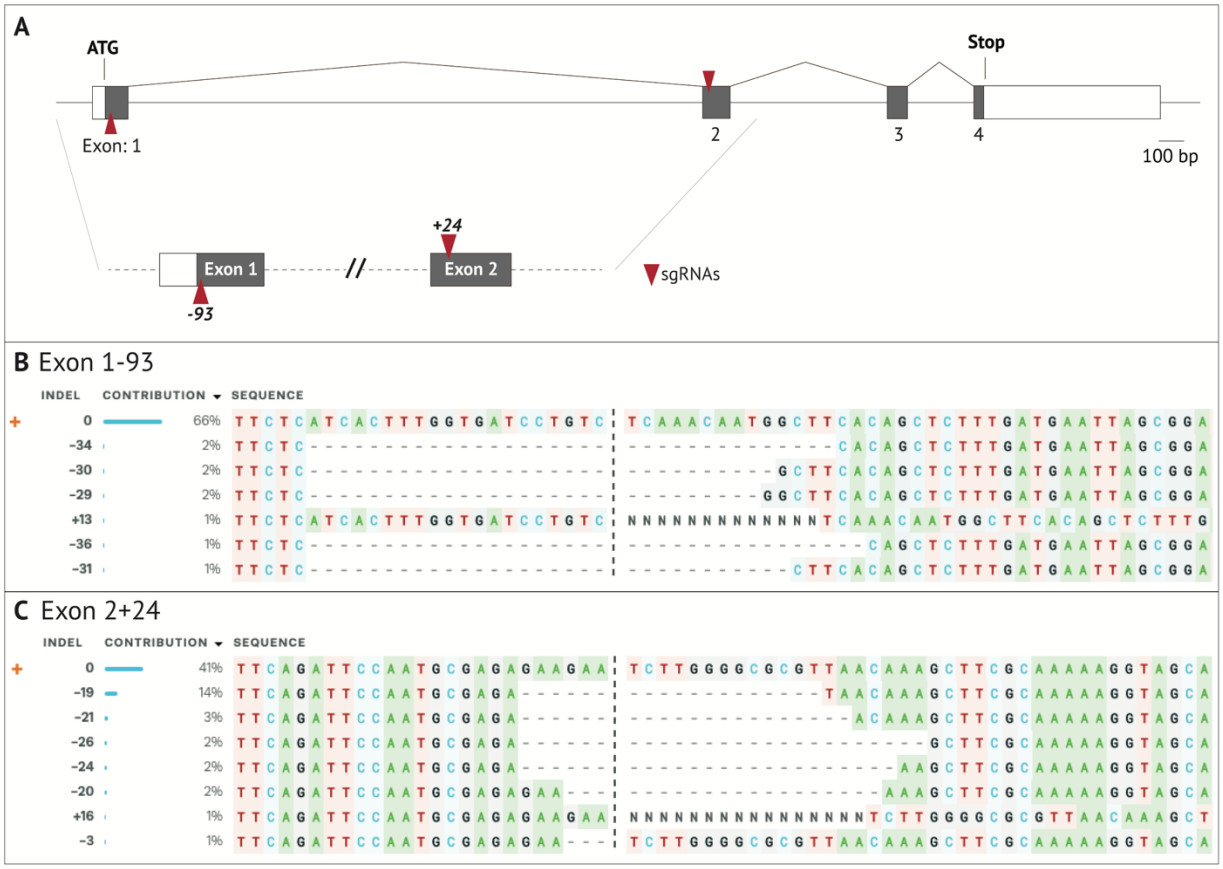

Figure 9. CRISPR/Cas9 guide design and validation. (A) Genomic model of LpStrongylocin 2. Red arrows mark the single guide RNA target region. Guides were generated to target Exon 1 and 2. **(B,C)** Example of indels generated within a single larva from sgRNA Exon 1-93 and Exon 2+24. **(B)** and **(C)** are sequences from different individuals. + indicates the wild type sequence.

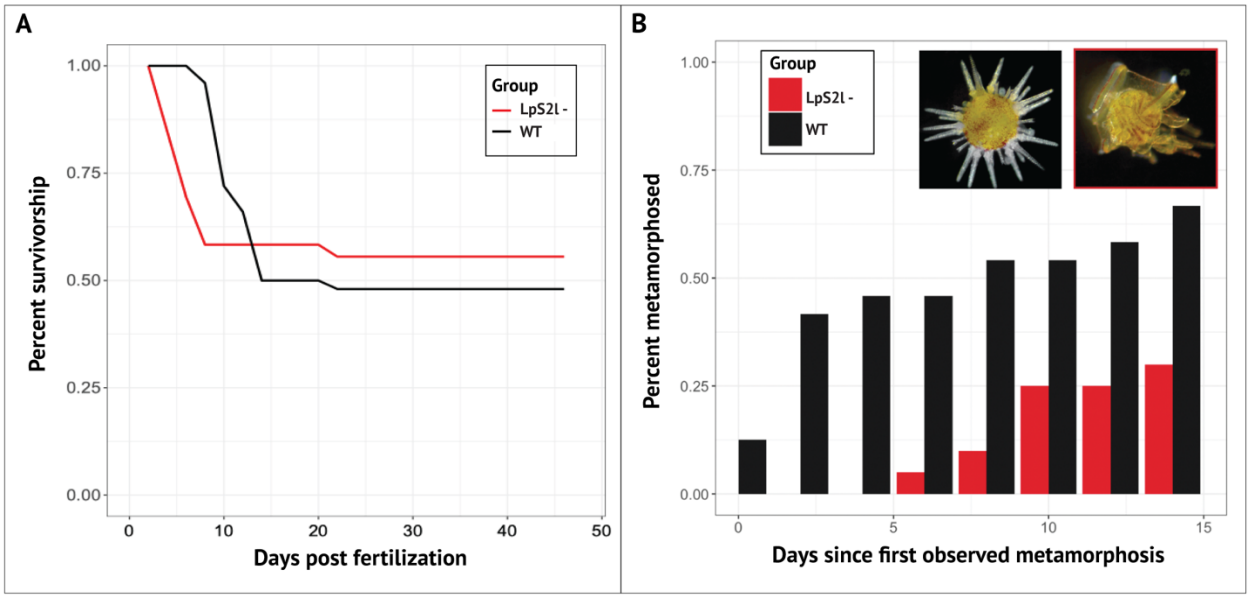

Figure 10. Survivorship and metamorphosis rates of *LpS2l*-disrupted and wild type larvae. **(A)** Survivorship rates of *LpS2l*- (red) and WT larvae (black). **(B)** Metamorphosis rates in WT (black, left image) and *LpS2l*- larvae (red, right image). Day 0 marks the first observation of metamorphosis. Day 15 marks the end of the observation period.

DISCUSSION

A homolog of *Strongylocin 2* is present in the *Lytechinus pictus* genome and is transcribed in response to bacterial challenge in early larvae.

Only one sea urchin specific antimicrobial peptide gene, *LpStrongylocin 2*, was found in the genome of *Lytechinus pictus*. The genome of *L. pictus* is slightly less expanded in comparison to species such as *S. purpuratus* which has both Centrocins (1 and 2) and Strongylocins (1 and 2) (Li et al., 2010), so this finding is not particularly surprising. Alternatively, there may be more divergent AMPs present in the genome that preclude discovery with the utilized BLAST approach. Domain-based searches (Buckley et al., 2019), as well as more improved whole genome sequencing updates, may yield more results in the future.

The predicted protein product of *LpS2l* is 98 aa. The conserved protospacer and cleavage regions found in *LpStrongylocin 2* indicate this peptide likely functions as an AMP. To test if *LpS2l* is transcribed during infection in a similar pattern to defensin-like AMPs in other organisms, a bacterial exposure assay was utilized. Prior to this study, the activity of *Strongylocin 2* transcription during a larval immune response was unknown in any sea urchin. This study found that *LpStrongylocin 2* transcription in *L. pictus* larvae is inducible with exposure to high concentrations of *Vibrio diazotrophicus*. This response is in line with the upregulation of many AMPs in other marine invertebrates following bacterial stimulation, such as with the manila clam *Ruditapes philippinarum,* which upregulates transcription of a defensin isophorm Rpdef1α upon stimulation with bacteria (Lv et al., 2020). The blue mussel *Mytilus galloprovincialis* was shown to synthesize and process *Mytilus galloprovincialis* defensin 1 (MGD1) in granulocytes, which are released into the protoplasm after bacterial stimulation (Mitta et al., 1999). The activation of *LpStrongylocin 2* transcription during bacterial exposure

implies a role in bacterial clearance within the gut as an active player in the larval immune system. Based on the known expression patterns of AMPs, I predict that larval *L. pictus* gut epithelial cells are being stimulated transcription and release *LpStrongylocin 2* into gut lumen to interact with invading bacteria. More specific co-stains with HCR could confirm the cell type transcribing *LpS2l* during infection. Further research should also explore the effectiveness and mechanisms of this peptide *in vivo* to clarify the role of this antimicrobial peptide during infection.

***LpStrongylocin 2* transcription is upregulated immediately prior to metamorphosis.**

Many AMPs in nature have pleiotropic roles in development that are less understood than their immune effector functions. Certain AMPs have been found to be developmentally regulated in some animals (Bruno et al., 2023, Fraune et al, 2010, Tapadia and Verma, 2012). In *Drosophila melanogaster,* multiple AMPs such as *diptercin, cecropinA, drosocin,* and *attacinA* only commence expression at the third instar stage— immediately prior to pupa stage and subsequent metamorphosis (Tapadia and Verma, 2012). This study found that in nascent larvae *LpStrongylocin 2* is not transcribed constitutively until the onset of developing rudiment structures in the final two stages of larval development. Given that other immune genes (*pks1, srcr142, IL17D)* are not upregulated in a similar pattern, I predict *LpS2l* is developmentally regulated as opposed to being transcribed in response to bacterial exposure at this stage. The later onset of *LpStrongylocin 2* immunocyte transcription is most likely employed in a developmental context rather than an immune response to increasing bacterial, however more specific studies should be conducted to explore the effect of various bacterial levels in laboratory cultures.

***LpStrongylocin 2* transcripts accumulate in predicted ameboid cells.**

Research has yet to adequately describe how the larval immune system changes throughout development as it approaches metamorphosis. The onset of *LpS2l* transcription as the larvae approaches the transition to the adult form presents an avenue for understanding the shift between the larval and adult immune system (Li et al., 2008). This work identified *LpS2l* transcripts accumulated in a subtype of blastocoelar cell. Based on the morphological resemblance and interactions with pigment cells, these *LpS2l*+ cells are likely ameboid cells. AMPs in other organisms are often transcribed in circulating phagocytic immune cells to clear engulfed bacteria (Bevins, 2007, Johnstone and Herzberg, 2012, Huttner and Berins, 1999). Interestingly, amoeboid cells have not been observed to phagocytose and the exact role of amoeboid cells in the larval immune response has yet to be defined. The presence of dense *LpS2l* transcripts in these cells implies the capability of amoeboid cells to indeed be phagocytic, or alternatively utilize AMPs for an alternative function such as immunomodulatory processes. In adults, Strongylocin 2 peptides are found in *S. droebachiensus* in red spherule cells, the adult counterpart of pigment cells, and phagocytes (Li et al., 2014). This disconnect in cell type specific expression is unexpected despite being in different species of urchin and further research should be done to isolate active LpStrongylocin 2 peptides from adult *L. pictus* coelomocytes. These results reveal the potential for different capabilities of larval and adult specific immune cells given stark differences in developmental processes and environmental requirements. Supported by developmental transcriptomic evidence of upregulation, *LpStrongylocin 2* may be transcribed prior to metamorphosis for its immunomodulatory abilities, utilized as a mechanism for amplifying signaling of certain bacterial presence or density.

***LpS2l* + cells are located within the tissue of developing structures in competent larvae.**

The localization patterns of *LpS2l* transcription in the rudiment and pedicellaria bring up an intriguing potential connection about the role of antimicrobial peptide signaling, stem cell differentiation, and tissue regeneration. In both vertebrates and invertebrates, immune cells play a key role in tissue regeneration and contribute to modulation of stem cell activation (Ballarin et al., 2021). Tissue resident macrophages in humans, for example, can regulate hemopoietic stem cell differentiation (Naik et al., 2018). Regeneration of the zebrafish brain is reliant on inflammation to stimulate neurogenesis through progenitor cell activation (Ballarin et al., 2021) The immunomodulatory capabilities of AMPs may be employed for signal amplification of bacterial presence to immune or surrounding cells, which may then interact with surrounding stem cells to initiate metamorphic processes. In the rudiment, developing tissue was shown to contain cells with accumulated *LpS2l* transcripts. These cells are predicted to be tissue resident ameboid cells and may utilize immune recognition processes to initiate developmental processes such as metamorphosis.

The presence of *LpS2l* in cells within the epidermal the tissue of the pedicellaria present a similar circumstance. As the pedicellariae develop, mesenchymal and skeletal cells migrate to the side of the soon to be pedicellaria and begin skeletal secretion (Burke, 1980). It is conceivable that cells with *LpS2l* transcripts are involved in the recruitment of cells for the development of new structures through signal recognition and cell-cell communication. Given that pedicellaria are external structures, an enticing hypothesis is that these cells may be involved in recognizing environmental bacteria and activating downstream processes initiating metamorphosis, potentially through the complement of neural and sensory cells on each jaw and base muscles (Burke et al., 2006). This potential relationship may be a link between

antimicrobial peptide signaling and nervous system pathways, although additional research is needed to explore this connection.

Immediately after metamorphosis, juveniles have transcriptional accumulation of *LpS2l* in cells on both the aboral and oral surfaces. The presence of antimicrobial peptides on the aboral decaying tissue has been observed in many species as a mechanism of preventing bacterial and fungal growth (Johnstone and Herzberg, 2022). Transcription on the oral surface is within the juvenile tissue may serve as a defense against infection during this morphological and ecological transition. Coelomocyte *LpS2l* transcription in juveniles can be assessed in the future by removing coelomic fluid and testing for transcripts within isolated coelomocytes.

The observed transcript accumulation of *LpS2l* in immune cells within developing structures opens the door to many questions regarding the role of tissue resident immune cells in developmental processes. The localization pattern observed in this study supports the role for this AMP in the metamorphic process. To further validate this candidate, future work should focus on understanding the interactions between active Strongylocin 2 and bacterial dsDNA, exploring the signal amplification and downstream pathway modulation capabilities of AMPs in the sea urchin.

FUTURE RESEARCH

Use of CRISPR/Cas9 guides for evaluating the role of LpStronglyocin 2 in the initiation of metamorphosis.

Using the CRISPR/Cas9 guides developed within this project, future experiments will be conducted to investigate the role of *LpS2l* in larval developmental processes. Given the results of this study and preliminary metamorphotic efficiency data, I hypothesize that larvae with functionally disrupted *LpS2l* will stall at metamorphic competency and fail to undergo metamorphosis. If this proves correct, exogenous rescue assays will be conducted to confirm the result is in fact evidence of *LpS2l* involvement in this process. However, genomic redundancy should always be considered when evaluating the effects of gene perturbation. If no decline in metamorphic efficiency is observed, other possible mechanisms of sensing bacterial cues should be investigated using techniques such as RNA-seq and qPCR to identify differentially transcribed genes in *LpS2l*-perturbed larvae. This research would potentially identify novel pathways involved in larval metamorphosis.

APPENDIX

Table S1. HCR probe sequences used in this study.

Probe name is the hairpin number followed by the Accession number of the top BLAST hit *S. purpuratus* sequence.

LOC129256550, XP_054750701.1, PREDICTED: *Lytechinus pictus* strongylocin 2-like	
Pool name	**Sequence**
B2_ XM_003725029.3	CCTCGTAAATCCTCATCAaaACTCATGTTGATATTTGCACAATAT
B2_ XM_003725029.4	AAATGTAATTTGTGTATATGAAATAaaATCATCCAGTAAACCGCC
B2_ XM_003725029.5	CCTCGTAAATCCTCATCAaaAGATTTAGCAAGAACGCAATTTAAT
B2_ XM_003725029.6	AAATAATCGTCTTTATTAATTAATCaaATCATCCAGTAAACCGCC
B2_ XM_003725029.7	CCTCGTAAATCCTCATCAaaCCTATCAATCGGACTTCTCTAATTT
B2_ XM_003725029.8	AAACTGTTATACCTCAATTATTATCaaATCATCCAGTAAACCGCC
B2_ XM_003725029.9	CCTCGTAAATCCTCATCAaaACTGCAGTTCAATAATTAGATTAAA
B2_ XM_003725029.10	TTTCATTAGGTTTACCGATTGTACCaaATCATCCAGTAAACCGCC
B2_ XM_003725029.11	CCTCGTAAATCCTCATCAaaGTTCGCCATCACCATCCATCATCGT
B2_ XM_003725029.12	AAAGATCCAAGGAGCATGTTACTGCaaATCATCCAGTAAACCGCC
B2_ XM_003725029.13	CCTCGTAAATCCTCATCAaaTGATACACGTACAAGCGATCTTGGT
B2_ XM_003725029.14	ATTACGAAACAAATTTCCTTCACTTaaATCATCCAGTAAACCGCC
B2_ XM_003725029.15	CCTCGTAAATCCTCATCAaaGGTGTGGTATTCTTCCCAAACACGA
B2_ XM_003725029.16	TAACTTGAAGTAACAGCTGTGCACGaaATCATCCAGTAAACCGCC
B2_ XM_003725029.17	CCTCGTAAATCCTCATCAaaTTTCATGCCCTCCTGTTGTTTGACA
B2_ XM_003725029.18	TATGACAGCAGATGTAATTTGCGCAaaATCATCCAGTAAACCGCC
B2_ XM_003725029.19	CCTCGTAAATCCTCATCAaaCATCATCCGCTAATTCATCAAAGAG
B2_ XM_003725029.20	CCCAAGATTCTTCTCTCGCATTGGAaaATCATCCAGTAAACCGCC
B2_ XM_003725029.21	CCTCGTAAATCCTCATCAaaCAAAGTGATGAGAAGAATGAAAGAT
B2_ XM_003725029.22	TGAAGCCATTGTTTGAGACAGGATCaaATCATCCAGTAAACCGCC
B2_ XM_003725029.23	CCTCGTAAATCCTCATCAaaTATCCAGGCACTGTCAGCTCTCTTA
B2_ XM_003725029.24	TTTGATGATATGCTTATTCTTGTTAaaATCATCCAGTAAACCGCC

Table S1. HCR probe sequences used in this study.

Probe name is the hairpin number followed by the Accession number of the top BLAST hit *S. purpuratus* sequence, *continued.*

LOC129277782, XP_054769928.1, PREDICTED: *Lytechinus pictus* uncharacterized	
Pool name	**Sequence**
B5_XM_788471.5	CTCACTCCCAATCTCTATaaCTTCTCCAAGAGGAGGCCAGTGGTG
B5_XM_788471.6	TCAGATGCAGACGTTATTGTCGATAaaCTACCCTACAAATCCAAT
B5_XM_788471.7	CTCACTCCCAATCTCTATaaCAAGCACCATCAAGAACTCTTCAAC
B5_XM_788471.8	GGGTATCAGGAGATAGAAGAAGTTTaaCTACCCTACAAATCCAAT
B5_XM_788471.9	CTCACTCCCAATCTCTATaaCCGGACGAATCTTCGCAGAGAGCAT
B5_XM_788471.10	TTTCTGACATGACGTGTGACAGCTTaaCTACCCTACAAATCCAAT
B5_XM_788471.11	CTCACTCCCAATCTCTATaaGACTTTGTTTGGTTTGAATGCTGAT
B5_XM_788471.12	TTTCTTGAAGAGTTGTGTCGTTGAGaaCTACCCTACAAATCCAAT
B5_XM_788471.13	CTCACTCCCAATCTCTATaaAGTCGGTGATTGAACAGAAGCGTCC
B5_XM_788471.14	TCTGTAGTTTGAAATTGATAGCATTaaCTACCCTACAAATCCAAT
B5_XM_788471.15	CTCACTCCCAATCTCTATaaCAGGCTGTAGTATGTAGTTGCAAAG
B5_XM_788471.16	CCCATTTGTGATGTTAGCTCTTTCAaaCTACCCTACAAATCCAAT
B5_XM_788471.17	CTCACTCCCAATCTCTATaaTCCTCTACTGACGACTCTGTCTTGA
B5_XM_788471.18	AACCCATCTTGGTATGCGATGCCCAaaCTACCCTACAAATCCAAT
B5_XM_788471.19	CTCACTCCCAATCTCTATaaCCATCCATAGCTTGCAAACGTTCTC
B5_XM_788471.20	TTGGTCCCGAAGTGGCAGCAAAGGTaaCTACCCTACAAATCCAAT
B5_XM_788471.21	CTCACTCCCAATCTCTATaaGCTTTGGGATTTATGCAAGCATCAT
B5_XM_788471.22	CATTGCTTGCGTGTGGTGACTGGTGaaCTACCCTACAAATCCAAT
B5_XM_788471.23	CTCACTCCCAATCTCTATaaATGTCGACTGATCCTGGGACGAACC
B5_XM_788471.24	GAGTGGAGTGTGTCCAAGCAGATCAaaCTACCCTACAAATCCAAT
B5_XM_788471.25	CTCACTCCCAATCTCTATaaCATCTCTGCTCCAGCCTTATAGTAG
B5_XM_788471.26	GAGAGCCTTGAGGACTGCCTGTCGTaaCTACCCTACAAATCCAAT
B5_XM_788471.27	CTCACTCCCAATCTCTATaaTGCAAGACAGATTGCTCCCATGTTT
B5_XM_788471.28	TACCTGTCCCAAACCATGCTTGATGaaCTACCCTACAAATCCAAT
B5_XM_788471.29	CTCACTCCCAATCTCTATaaGTGCCCAGCTGTCGCAATCAATGAT
B5_XM_788471.30	TCAAAGTAATCATGACATTTCCTCTaaCTACCCTACAAATCCAAT
B5_XM_788471.31	CTCACTCCCAATCTCTATaaCCCATTTCTTGCATGTATCCATAGA

Table S1. HCR probe sequences used in this study.

Probe name is the hairpin number followed by the Accession number of the top BLAST hit *S. purpuratus* sequence, *continued.*

LOC129277782, XP_054769928.1, PREDICTED: *Lytechinus pictus* uncharacterized	
Pool name	**Sequence**
B5_XM_788471.32	ACCTGGAACTTGGCACCATATTCGAaaCTACCCTACAAATCCAAT
B5_XM_788471.33	CTCACTCCCAATCTCTATaaACTCGACATATCCAGACTCTGGAAA
B5_XM_788471.34	TTTCACCACTGGTGGCTTCCATGATaaCTACCCTACAAATCCAAT
B5_XM_788471.35	CTCACTCCCAATCTCTATaaGCACACATGCGGTCATCCTGGTTTC
B5_XM_788471.36	TTGTGCATGTTACCAAGGGATCGAAaaCTACCCTACAAATCCAAT
B5_XM_788471.37	CTCACTCCCAATCTCTATaaACGCAGTTGTTTGGCAATGGTTGGG
B5_XM_788471.38	GTCTGGTGTATGGAAGGCACACTGGaaCTACCCTACAAATCCAAT
B5_XM_788471.39	CTCACTCCCAATCTCTATaaTCAACCGCTTCTTCAAGGGTCATCC
B5_XM_788471.40	TGCTCCACGCTCCTGATGTAGATGGaaCTACCCTACAAATCCAAT
B5_XM_788471.41	CTCACTCCCAATCTCTATaaTCTTCTTAAAGATGGCATCGCATTC
B5_XM_788471.42	TTTCTTCGAGGACGGACCAACCACTaaCTACCCTACAAATCCAAT
B5_XM_788471.43	CTCACTCCCAATCTCTATaaTCCAGGAGACTACACTCATGGCATC
B5_XM_788471.44	TTTCATGAAGTCGACGTCTGGTGGAaaCTACCCTACAAATCCAAT
B5_XM_788471.45	CTCACTCCCAATCTCTATaaGGCAAACCCAAAGGAGTTGAGGCCG
B5_XM_788471.46	CTCGAAGATACAATGGGCCAGTGCTaaCTACCCTACAAATCCAAT
B5_XM_788471.47	CTCACTCCCAATCTCTATaaTCTGCTTCTAGAGGATCACCAACCA
B5_XM_788471.48	GGGCGGTCGAATGCCTTGGAGATGGaaCTACCCTACAAATCCAAT
B5_XM_788471.49	CTCACTCCCAATCTCTATaaTAGCGGTACTTGAGAAGGGACTGCA
B5_XM_788471.50	CCCATCCTTCACTGCGCACGTATCCaaCTACCCTACAAATCCAAT
B5_XM_788471.51	CTCACTCCCAATCTCTATaaATAAGAGATACGATTAGCCGACACA
B5_XM_788471.52	AAAGGATGGACCTTTGAGGTTGAATaaCTACCCTACAAATCCAAT
B5_XM_788471.53	CTCACTCCCAATCTCTATaaTCAAAGCCATCCATGTCCTCGATGA
B5_XM_788471.54	CGAGGTGAAATCTTGAAGAAGAGGTaaCTACCCTACAAATCCAAT

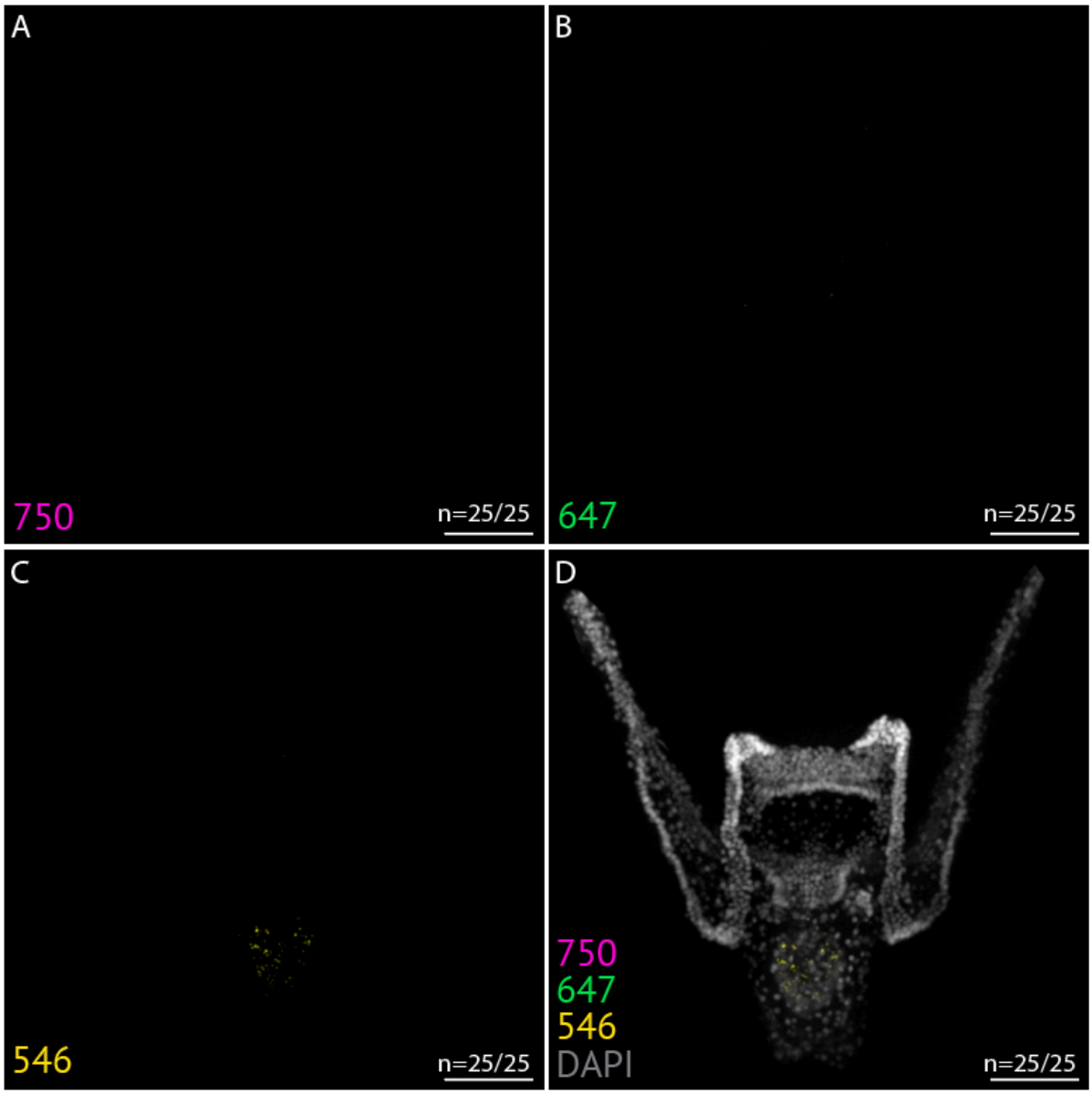

Figure S1. Negative controls of 3dpf larvae. (A-C) Fluorescent channels of the same no-probe larval sample with only hairpins added. Non-specific signal was present only in the 546 nm channel. **(D)** Merged fluorescent channels with DAPI nuclear stain overlay. Scale bar= 50µm.

REFERENCES

Alker, A. T., Farrell, M. V., Demko, A. M., Purdy, T. N., Adak, S., Moore, B. S., Sneed, J. M., Paul, V. J., & Shikuma, N. J. (2023). Linking bacterial tetrabromopyrrole biosynthesis to coral metamorphosis. *bioRxiv : the preprint server for biology*, 2023.05.08.539906. https://doi.org/10.1101/2023.05.08.539906Altschul SF, Gish W, Miller W, Myers EW, Lipman DJ. Basic local alignment search tool. *J Mol Biol*. 1990;215(3):403-410. doi:10.1016/S0022-2836(05)80360-2

Arshinoff BI, Cary GA, Karimi K, Foley S, Agalakov S, Delgado F, Lotay VS, Ku CJ, Pells TJ, Beatman TR, Kim E, Cameron RA, Vize PD, Telmer CA, Croce J, Ettensohn CA, Hinman VF, Echinobase: leveraging an extant model organism database to build a knowledgebase supporting research on the genomics and biology of echinoderms, *Nucleic Acids Research*, Volume 50, Issue D1, 2022, 10.1093/nar/gkab1005

Ballarin, L., Karahan, A., Salvetti, A., Rossi, L., Manni, L., Rinkevich, B., Rosner, A., Voskoboynik, A., Rosental, B., Canesi, L., Anselmi, C., Pinsino, A., Tohumcu, B. E., Jemec Kokalj, A., Dolar, A., Novak, S., Sugni, M., Corsi, I., & Drobne, D. (2021). Stem Cells and Innate Immunity in Aquatic Invertebrates: Bridging Two Seemingly Disparate Disciplines for New Discoveries in Biology. Frontiers in immunology, 12, 688106. https://doi.org/10.3389/fimmu.2021.688106

Bevins C. L. (1994). Antimicrobial peptides as agents of mucosal immunity. Ciba Foundation symposium, 186, 250–269. https://doi.org/10.1002/9780470514658.ch15

Blyth, G. (2022). Regulation of colonic mucus and epithelial cell barrier function by cathelicidin (Doctoral thesis, University of Calgary, Calgary, Canada). Retrieved from https://prism.ucalgary.ca. http://hdl.handle.net/1880/114687.

Bruno, R., Boidin-Wichlacz, C., Melnyk, O., Zeppilli, D., Landon, C., Thomas, F., Cambon, M. A., Lafond, M., Mabrouk, K., Massol, F., Hourdez, S., Maresca, M., Jollivet, D., & Tasiemski, A. (2023). The diversification of the antimicrobial peptides from marine worms is driven by environmental conditions. The Science of the total environment, 879, 162875. https://doi.org/10.1016/j.scitotenv.2023.162875 Buckley KM, Ho ECH, Hibino T, et al. IL17 factors are early regulators in the gut epithelium during inflammatory response to *Vibrio* in the sea urchin larva. *Elife*. 2017;6:e23481. Published 2017 Apr 27. doi:10.7554/eLife.23481

Buckley KM, Rast JP. Dynamic evolution of toll-like receptor multigene families in echinoderms. *Front Immunol*. 2012;3:136. Published 2012 Jun 5. doi:10.3389/fimmu.2012.00136

Buckley KM, Schuh NW, Heyland A, Rast JP. Analysis of immune response in the sea urchin larva. *Methods Cell Biol*. 2019;150:333-355. doi:10.1016/bs.mcb.2018.10.009

Burke, R. D., Angerer, L. M., Elphick, M. R., Humphrey, G. W., Yaguchi, S., Kiyama, T., Liang, S., Mu, X., Agca, C., Klein, W. H., Brandhorst, B. P., Rowe, M., Wilson, K.,

Churcher, A. M., Taylor, J. S., Chen, N., Murray, G., Wang, D., Mellott, D., Olinski, R., F. Hallböök, Thorndyke, M. C. (2006). A genomic view of the sea urchin nervous system. Developmental biology, 300(1), 434–460. https://doi.org/10.1016/j.ydbio.2006.08.007

Burke RD, 1980. Development of pedicellariae in the pluteus larva of Lytechinus pictus (Echinodermata: Echinoidea). Canadian Journal of Zoology. 58(9): 1674-1682. https://doi.org/10.1139/z80-229

Cameron RA, Hinegardner RT. Initiation of metamorphosis in laboratory cultured sea urchins. Biol Bull. 1974;146(3):335-342. doi:10.2307/1540409

Cavalcanti GS, Alker AT, Delherbe N, Malter KE, Shikuma NJ. The Influence of Bacteria on Animal Metamorphosis. *Annu Rev Microbiol*. 2020;74:137-158. doi:10.1146/annurev-micro-011320-012753

Choi, H. M. T., Schwarzkopf, M., Fornace, M. E., Acharya, A., Artavanis, G., Stegmaier, J., Cunha, A., & Pierce, N. A. (2018). Third-generation in situ hybridization chain reaction: multiplexed, quantitative, sensitive, versatile, robust. Development (Cambridge, England), 145(12), dev165753. https://doi.org/10.1242/dev.165753

Deatherage, L., Cookson, B. T. Membrane vesicle release in bacteria, eukaryotes, and archaea: A conserved yet underappreciated aspect of microbial life. Infect. Immun. 80, 1948–1957 (2012).

Doll, Peter C., Caballes, Ceimon F., Hoey, Andrew S., Uthicke, Sven, Ling, Scott D., Pratchett, Morgan S. "Larval Settlement in Echinoderms: A Review of Processes and Patterns." *Oceanography and Marine Biology. an Annual Review*, Taylor & Francis, Boca Raton, FL, 2023, pp. 433–494.

Dworjanyn SA, Pirozzi I (2008) Induction of settlement in the sea urchin Tripneustes gratilla by macroalgae, biofilms, and conspecifics: a role for bacteria? Aquaculture 274: 268–274

Edelman GM, Gally JA. Degeneracy and complexity in biological systems. Proc Natl Acad Sci U S A. 2001;98(24):13763-13768. doi:10.1073/pnas.231499798

Fleming, T. J., Schrankel, C. S., Vyas, H., Rosenblatt, H. D., & Hamdoun, A. (2021). CRISPR/Cas9 mutagenesis reveals a role for ABCB1 in gut immune responses to Vibrio diazotrophicus in sea urchin larvae. The Journal of experimental biology, 224(7), jeb232272. https://doi.org/10.1242/jeb.232272

Fraune, S.; Augustin, R.; Anton-Erxleben, F.; Wittlieb, J.; Gelhaus, C.; Klimovich, V.B.; Samoilovich, M.P.; Bosch, T.C. In an early branching metazoan, bacterial colonization of the embryo is controlled by maternal antimicrobial peptides. *Proc. Natl. Acad. Sci. USA* 2010, *107*, 18067–18072.

Freckelton, M., Nedved, B. & Hadfield, M. Induction of Invertebrate Larval Settlement; Different Bacteria, Different Mechanisms?. *Sci Rep* **7**, 42557 (2017). https://doi.org/10.1038/srep42557

Ganz T, Rayner JR, Valore EV, Tumolo A, Talmadge K, Fuller F. The structure of the rabbit macrophage defensin genes and their organ-specific expression. *J Immunol*. 1989;143(4):1358-1365.

Guryanova SV, Balandin SV, Belogurova-Ovchinnikova OY, Ovchinnikova TV. Marine Invertebrate Antimicrobial Peptides and Their Potential as Novel Peptide Antibiotics. *Mar Drugs*. 2023;21(10):503. Published 2023 Sep 23. doi:10.3390/md21100503

Hadfield MG. Biofilms and marine invertebrate larvae: what bacteria produce that larvae use to choose settlement sites. *Ann Rev Mar Sci*. 2011;3:453-470. doi:10.1146/annurev-marine-120709-142753

Hinegardner, R. T. (1969). Growth and development of the laboratory cultured sea urchin. *The Biological Bulletin*, *137*(3), 465-475.

Hinegardner, R. T. (1975). Morphology and Genetics of Sea-Urchin Development. *American Zoologist*, *15*(3), 679–689. http://www.jstor.org/stable/3882087

Hirano M. (2016). Echinoderm immunity: is the larval immune system immature?. Immunology and cell biology, 94(9), 809–811. https://doi.org/10.1038/icb.2016.67

Huan Y, Kong Q, Mou H, Yi H. Antimicrobial Peptides: Classification, Design, Application and Research Progress in Multiple Fields. *Front Microbiol*. 2020;11:582779. Published 2020 Oct 16. doi:10.3389/fmicb.2020.582779

Huggett, M. J., Williamson, J. E., De Nys, R. S., Kjelleberg and P. D. Steinberg, Oecologia, 2006, 149, 604–619, DOI: 10.1007/s00442-006-0470-8.

Huttner KM, Brezinski-Caliguri DJ, Mahoney MM, Diamond G. Antimicrobial peptide expression is developmentally regulated in the ovine gastrointestinal tract. J Nutr. 1998;128(2 Suppl):297S-299S. doi:10.1093/jn/128.2.297S

Huttner, K. M., & Bevins, C. L. (1999). Antimicrobial peptides as mediators of epithelial host defense. Pediatric research, 45(6), 785–794. https://doi.org/10.1203/00006450-199906000-00001

Ho, E., Buckley, K. M., Schrankel, C. S., Schuh, N. W., Hibino, T., Solek, C. M., Bae, K., Wang, G., & Rast, J. P. (2016). Perturbation of gut bacteria induces a coordinated cellular immune response in the purple sea urchin larva. *Immunology and cell biology*, *94*(9), 861–874. https://doi.org/10.1038/icb.2016.51

Hyman, L. H., 1955. The Invertebrates: Echinodermata. The Coelomate Bilateria. Vol. IV. McGraw-Hill Book Company, Inc., New York, 763

Johnstone, K. F., & Herzberg, M. C. (2022). Antimicrobial peptides: Defending the mucosal epithelial barrier. Frontiers in oral health, 3, 958480. https://doi.org/10.3389/froh.2022.958480

Labun, K., Montague, T. G., Gagnon, J. A., Thyme, S. B., & Valen, E. (2016). CHOPCHOP v2: a web tool for the next generation of CRISPR genome engineering. Nucleic acids research, 44(W1), W272–W276. https://doi.org/10.1093/nar/gkw398

Li, C., Haug, T., Styrvold, O. B., Jørgensen, T. Ø., & Stensvåg, K. (2008). Strongylocins, novel antimicrobial peptides from the green sea urchin, Strongylocentrotus droebachiensis. Developmental and comparative immunology, 32(12), 1430–1440. https://doi.org/10.1016/j.dci.2008.06.013

Li C, Blencke HM, Smith LC, Karp MT, Stensvåg K. Two recombinant peptides, SpStrongylocins 1 and 2, from Strongylocentrotus purpuratus, show antimicrobial activity against Gram-positive and Gram-negative bacteria. *Dev Comp Immunol*. 2010;34(3):286-292. doi:10.1016/j.dci.2009.10.006

Li, C., Blencke, H. M., Haug, T., Jørgensen, Ø., & Stensvåg, K. (2014). Expression of antimicrobial peptides in coelomocytes and embryos of the green sea urchin (Strongylocentrotus droebachiensis). Developmental and comparative immunology, 43(1), 106–113. https://doi.org/10.1016/j.dci.2013.10.013

Li, C., Haug, T., & Stensvåg, K. (2010). Antimicrobial peptides in Echinoderms. *Invertebrate Survival Journal*, *7*(1), 132-140.

Li C, Haug T, Moe MK, Styrvold OB, Stensvåg K. Centrocins: isolation and characterization of novel dimeric antimicrobial peptides from the green sea urchin, Strongylocentrotus droebachiensis. *Dev Comp Immunol*. 2010;34(9):959-968. doi:10.1016/j.dci.2010.04.004

Lee EY, Lee MW, Wong GCL. Modulation of toll-like receptor signaling by antimicrobial peptides. *Semin Cell Dev Biol*. 2019;88:173-184. doi:10.1016/j.semcdb.2018.02.002

Lv C, Han Y, Yang D, Zhao J, Wang C, Mu C. Antibacterial activities and mechanisms of action of a defensin from manila clam Ruditapes philippinarum. *Fish Shellfish Immunol*. 2020;103:266-276. doi:10.1016/j.fsi.2020.05.025

Lyons, D. C., Kaltenbach, S. L., & McClay, D. R. (2012). Morphogenesis in sea urchin embryos: linking cellular events to gene regulatory network states. *Wiley interdisciplinary reviews. Developmental biology*, *1*(2), 231–252. https://doi.org/10.1002/wdev.18

Mahlapuu, M., Håkansson, J., Ringstad, L., & Björn, C. (2016). Antimicrobial Peptides: An Emerging Category of Therapeutic Agents. *Frontiers in cellular and infection microbiology*, *6*, 194. https://doi.org/10.3389/fcimb.2016.00194.

Mitta G, Vandenbulcke F, Hubert F, Roch P. Mussel defensins are synthesised and processed in granulocytes then released into the plasma after bacterial challenge. *J Cell Sci*. 1999;112 (Pt 23):4233-4242. doi:10.1242/jcs.112.23.4233

Naik, S., Larsen, S. B., Cowley, C. J., & Fuchs, E. (2018). Two to tango: dialog between immunity and stem cells in health and disease. *Cell*, *175*(4), 908-920.

Nesbit, K. T., Fleming, T., Batzel, G., Pouv, A., Rosenblatt, H. D., Pace, D. A., Hamdoun, A., & Lyons, D. C. (2019). The painted sea urchin, Lytechinus pictus, as a genetically-enabled developmental model. *Methods in cell biology*, *150*, 105–123. https://doi.org/10.1016/bs.mcb.2018.11.010.

Null, R. insitu_probe_generator. Zenodo. https://doi.org/10.5281/zenodo.3871970 (2021)

Otero-González, A. J., Magalhães, B. S., Garcia-Villarino, M., López-Abarrategui, C., Sousa, D. A., Dias, S. C., & Franco, O. L. (2010). Antimicrobial peptides from marine invertebrates as a new frontier for microbial infection control. FASEB journal : official publication of the Federation of American Societies for Experimental Biology, 24(5), 1320–1334. https://doi.org/10.1096/fj.09-143388

Pearce CM, Scheibling RE. Induction of Metamorphosis of Larvae of the Green Sea Urchin, Strongylocentrotus droebachiensis, by Coralline Red Algae. Biol Bull. 1990;179(3):304-311. doi:10.2307/1542322

Pettersen, E. F., Goddard, T. D., Huang, C. C., Meng, E. C., Couch, G. S., Croll, T. I., Morris, J. H., & Ferrin, T. E. (2021). UCSF ChimeraX: Structure visualization for researchers, educators, and developers. Protein science : a publication of the Protein Society, 30(1), 70–82. https://doi.org/10.1002/pro.3943Rischer M., Guo H. J., Beemelmanns C. (2022). Signalling molecules inducing metamorphosis in marine organisms. Nat. Prod. Rep. 39 (9), 1833–1855. doi: 10.1039/d1np00073j

Sea Urchin Genome Sequencing Consortium (2006). The genome of the sea urchin Strongylocentrotus purpuratus. Science (New York, N.Y.), 314(5801), 941–952. https://doi.org/10.1126/science.1133609

Shikuma NJ, Pilhofer M, Weiss GL, Hadfield MG, Jensen GJ, Newman DK. Marine tubeworm metamorphosis induced by arrays of bacterial phage tail-like structures. Science. 2014 Jan 31;343(6170):529-33. doi: 10.1126/science.1246794. Epub 2014 Jan 9. PMID: 24407482; PMCID: PMC4949041.

Smith, L. C., Arizza, V., Barela Hudgell, M. A., Barone, G., Bodnar, A. G., Buckley, K. M., Cunsolo, V., Dheilly, NM., Franchi, N., Fugmann, SD., Furukawa, R., Garcia-Arraras, J., Henson, JH., Hibino, T., Irons, ZH., Li, C., Lun, CM., Majeske, AJ., Oren, M., Pagliara, P., Pinsino, A., Raftos, DA., Rast, JP., Samasa, B., Schillaci, D., Schrankel, CS., Stabili, L., Stensväg, K., Sutton, E. (2018). Echinodermata: the complex immune system in echinoderms. *Advances in comparative immunology*, 409-501.

Solstad, R. G., Li, C., Isaksson, J., Johansen, J., Svenson, J., Stensvåg, K., & Haug, T. (2016). Novel Antimicrobial Peptides EeCentrocins 1, 2 and EeStrongylocin 2 from the Edible Sea Urchin Echinus esculentus Have 6-Br-Trp Post-Translational Modifications. PloS one, 11(3), e0151820. https://doi.org/10.1371/journal.pone.0151820

Swanson RL, Marshall DJ, Steinberg PD. Larval desperation and histamine: how simple responses can lead to complex changes in larval behaviour. *J Exp Biol*. 2007;210(Pt 18):3228-3235. doi:10.1242/jeb.004192

Verma, P., & Tapadia, M. G. (2012). Immune response and anti-microbial peptides expression in Malpighian tubules of Drosophila melanogaster is under developmental regulation. PloS one, 7(7), e40714. https://doi.org/10.1371/journal.pone.0040714

Umnyakova, E.S.; Gorbunov, N.P.; Zhakhov, A.V.; Krenev, I.A.; Ovchinnikova, T.V.; Kokryakov, V.N.; Berlov, M.N. Modulation of Human Complement System by Antimicrobial Peptide Arenicin-1 from Arenicola marina. *Mar. Drugs* 2018, *16*, 480.

Vyas, H., Schrankel, C. S., Espinoza, J. A., Mitchell, K. L., Nesbit, K. T., Jackson, E., Chang, N., Lee, Y., Warner, J., Reitzel, A., Lyons, D. C., & Hamdoun, A. (2022). Generation of a homozygous mutant drug transporter (ABCB1) knockout line in the sea urchin Lytechinus pictus. Development (Cambridge, England), 149(11), dev200644. https://doi.org/10.1242/dev.200644

Williamson JE, de Nys R, Kumar N, Carson DG, Steinberg PD (2000) Induction of metamorphosis in the sea urchin Holopneustes purpurascens by a metabolite complex from the algal host Delisea pulchra. Biol Bull 198:332–345

Wimley W. C. (2010). Describing the mechanism of antimicrobial peptide action with the interfacial activity model. *ACS chemical biology*, *5*(10), 905–917. https://doi.org/10.1021/cb1001558

Wynen H, Taylor E, Heyland A. Thyroid hormone-induced cell death in sea urchin metamorphic development. *J Exp Biol*. 2022;225(23):jeb244560. doi:10.1242/jeb.244560

Zasloff, M. Antimicrobial peptides of multicellular organisms. Nature 415, 389–395 (2002). https://doi.org/10.1038/415389a

Zhang, Q. Y., Yan, Z. B., Meng, Y. M., Hong, X. Y., Shao, G., Ma, J. J., Cheng, X. R., Liu, J., Kang, J., & Fu, C. Y. (2021). Antimicrobial peptides: mechanism of action, activity and clinical potential. *Military Medical Research*, *8*(1), 48. https://doi.org/10.1186/s40779-021-00343-2